Dynamics of ion storage processes in electron beams and rings

É. A. Perel'shteĭn and G. D. Shirkov

Joint Institute for Nuclear Research, Dubna

Fiz. Elem. Chastits At. Yadra **18**, 154–197 (January–February 1987)

This review is devoted to processes in electron-ion beams and rings. The fundamentals of the distribution-function moments method in electron-ion beam physics and its applications to the dynamics of multicomponent beams with noncoincident dimensions are presented. Ion production and storage in electron-beam sources and in the electron rings of the collective accelerator are studied. A new type of highly charged ion source using a supplementary compression ring in a collective accelerator is discussed.

INTRODUCTION

The history of the nuclear physics of heavy ions begins about thirty years ago. The results of experiments in heavy-ion beams obtained at the cyclotron of the Institute of Atomic Energy were first presented in 1957.[1] In later years heavy-ion physics developed intensively in two directions. Traditionally, the properties of nuclear matter at low and intermediate energies have been studied along with the synthesis of transuranium elements. During the last ten years, A. M. Baldin at Dubna has been the leader in the creation of a new, broad scientific area—relativistic nuclear physics. Beams of relativistic nuclei provide a powerful tool for studying high-energy physics, in particular, for verifying the basic ideas of quark models and quantum chromodynamics.[2]

Aside from charged-particle accelerators, ion beams are used in various areas of science and technology. Here we shall only briefly list the main areas: studies of controlled thermonuclear fusion, atomic physics, including the spectroscopy of highly charged ions, lasers, and astrophysical studies. The use of ion beams for applied research is constantly becoming more widespread, particularly in medicine, in radio electronics, and in the manufacture of nuclear filters.

The list of applications of highly charged ion beams could be made even longer. The essential feature is the fact that the number of fundamental and applied problems whose solution involves the use of ions of various elements is constantly growing.

Various types of ion sources have been developed for ion production. Most of them are based on the heating and confinement of a high-temperature plasma. Examples are the plasma-arc source or the Penning source, the duoplasmotron and the source based on the electron-cyclotron resonance. In a laser source an ion beam is generated from the plasma produced as the result of the interaction of the laser radiation with the working substance. The principles of the operation and construction of these devices can be found, for example, in Refs. 3–5. The maximum charges of the heavy ions obtained in this manner do not exceed 15–20. Ionization of the inner atomic shells requires that the plasma temperature exceed the binding energy of K and L electrons, which for heavy elements reaches tens of keV, and that the Lawson parameter (the product of the plasma density n and the confinement time τ) be $n\tau = 10^{12}$–10^{13} cm^{-3}·sec. The complete stripping of uranium nuclei requires $n\tau \sim 10^{14}$ cm^{-3}·sec at a plasma temperature of about 200 keV. It is as difficult to solve this problem as to solve the problem of controlled thermonuclear fusion.

The use of electron beams with high charge density has proved to be more useful in sources of highly charged ions of heavy elements. It is easy to focus an electron beam by means of external electromagnetic fields, and the ions are trapped in the potential well of the electron charge itself. E. D. Donets at Dubna has, on the basis of this principle, developed an electron-beam ionizer[6] or, as it is now referred to, the EBIS (Electron Beam Ion Source). Ion sources of the EBIS type have become widespread in recent years and are used as ion injectors in accelerators. Record values of heavy-ion charges have been obtained in them. For example, Xe^{52+} ions have been detected in the source KRION-2.[7]

Twenty years ago at Dubna, V. I. Veksler and V. P. Sarantsev led in the development of a new area of accelerator physics—the collective method of ion acceleration by electron rings.[8] A dense ring of relativistic electrons is used for this purpose. When the ring is accelerated, the ions are contained by the electron fields. As a result, it is possible to obtain an ion acceleration rate which is several times that obtained by traditional methods. Since 1977 experiments on the acceleration of ions of various elements have been carried out at the JINR heavy-ion collective accelerator (HICAC).[9] The electron rings of the HICAC can also be used to obtain highly charged ions.[10,11] The plans call for the nuclotron, the new relativistic-nucleus accelerator at the JINR, to be used as the injector in the collective accelerator HICAC-20 presently under construction.[12]

The ion production and storage processes in the electron beams of the EBIS and the electron rings of the HICAC are similar. Ions are produced from neutral atoms as a result of electron collisions and are confined in the potential well of the electron charge. Their charge is increased by successive collisions. The electron density and duration of the electron beam in the EBIS or the confinement time of the electron ring in the HICAC are sufficient for obtaining highly charged ions.

In recent years special attention has been paid to the problems of ion storage and the dynamics of multicomponent electron-ion beams. A large number of theoretical, computational, and experimental studies have been published. The method of the total moments of the distribution function in the dynamics of charged-particle beams has proved particularly sucessful in solving these problems.[13,14] Many processes involving ions in linear and circular beams of duration 10^{-4}–10 sec have been studied and analyzed. The present article is devoted to a systematic review of these studies.

 0090-4759/87/010064-19$04.40

We note that, owing to their extremely short duration (10^{-8}–10^{-6} sec), the nature of ion storage in high-current and relativistic electron beams and in the collective acceleration of ions by direct electron beams is considerably different from processes occurring in the EBIS and HICAC. These questions have been studied in Refs. 15–19.

1. ION PRODUCTION AND STORAGE IN ELECTRON BEAMS AND RINGS

Ion production

In electron beams ions are produced from neutral atoms (molecules) of the residual gas in the region where the beam propagates or in the injection of a neutral jet into the beam volume. The initial ion energy is equal to the energy of the neutral atoms, i.e., it is somewhere near the thermal energy. Therefore, the produced ions are confined in the potential well of the electron charge even in relatively rarefied beams of electron linear density 10^7–10^8 cm^{-1}. It is possible in principle to inject ions directly into the beam. It follows from energy–momentum conservation that in stationary electromagnetic fields the only ions which remain in the potential well are those whose charge has increased in passing through the beam. In EBIS-type sources ions from the ionization region are injected into the trap by removal of the external potential barrier.

Two ionization mechanisms are important in the electron-ion beams under consideration. The first is ionization of neutral atoms and ions by electron collisions. The second is the production of new ions in charge exchange between highly charged ions and neutral atoms. As a rule, the cross sections for the ionization of neutral atoms by ions moving in the potential well of the beam are very low and this process does not affect the overall picture.

The produced ions remain inside the volume of the electron beam and can undergo further ionization. The accumulated ions interact with each other and with the neutral gas in the beam. Aside from special cases, several of which will be discussed in detail below, the dominant process in electron-ion beams and rings is electron-ion ionization.

Ionization by electron collisions

Most of the original experimental and theoretical studies are devoted to the ionization of neutral atoms and ions by electron collisions. These questions have been discussed in considerable detail in the recent reviews of Refs. 7, 20, and 21. Here we shall consider only the main features of this process in electron beams. Collisions of electrons with neutral atoms and molecules lead to the production of positive ions. As a rule, molecular ions dissociate into separate charged ion fragments in subsequent collisions.[22]

In general, ionization processes can be divided into two groups. The direct ionization of an atom or ion can occur as the result of an interaction of the ionizing electron with one of the electrons of an outer subshell. The interaction of the electron with inner subshells leads to more complicated processes. A vacancy is produced after the excitation or ionization of an electron in an inner shell. The filling of the vacancy leads to the rearrangement of the entire atomic shell by transitions of the Auger or Coster–Kronig type with the emission of electrons from outer shells into the continuum. In the ionization of heavy elements, which have a complicated electronic shell structure, these processes are particularly important and the probability for them to occur is greater than the probability of double and multiple ionization.

The most important feature of the cross section for ionization by electron collisions is its threshold dependence on the collision energy E. Obviously, in order to strip an electron from a shell, the energy of the ionizing electron must be greater than the ionization energy I_k. The ionization cross section reaches its maximum value at $E = (2\text{–}3)I_k$. Many calculations have been carried out for various ion energy ranges and charge states.[20] A significant fraction of the calculations of the ionization cross section at nonrelativistic energies has been carried out using the classical Thomson formula[23]

$$\sigma_k^e = \frac{\pi n a_0^2}{I_k E}\left(1 - \frac{I_k}{E}\right), \qquad (1)$$

where I_k and E are the ionization and collision energies in atomic units (1 a.u. = 27.21 eV), n is the number of electrons in the outer shell, and a_0 is the Bohr radius. The calculated values of the ionization potentials for ions of all the elements are given, for example, in Ref. 24.

The most complete experimental study of the ionization cross sections of various charge states of ions of gaseous elements in the ionization energy range up to 18 keV has been carried out by E. D. Donets using an electron-beam ion source. Of particular interest are the ionization cross sections for hydrogen-like ions up to Ar^{17+} inclusive shown in Fig. 1,[25,26] which are in good agreement with the calculated values.[27] In Fig. 1 the ionization cross section σ_e is given in the form of a universal dependence on the nucleus charge Z, and the electron energies E are divided by the ionization energy I.

The cross sections for ionization by relativistic electrons have been calculated relatively recently for several gaseous elements[28–30] and for uranium.[30] The cross sections for direct ionization can be estimated using the expression of Ref. 31:

$$\sigma_k^e = \pi n r_e^2 \frac{mc^2}{I_k} \ln\left(\frac{E}{I_k}\right), \qquad (2)$$

where m and $r_e = e^2/mc^2$ are the electron mass and classical radius, e is the electron charge, and c is the speed of light. The cross sections for direct ionization of neutral Kr and Xe atoms by electrons of energy 0.5–3 MeV have been measured experimentally.[32] The direct-ionization cross sections calculated in Ref. 30 agree most closely with experiment. The cross sections for Auger ionization of internal shells of heavy elements[28,29] are comparable and in some cases even larger than those for direct ionization. In Fig. 2 we give the total cross section for ionization of Xe ions obtained by summing their cross sections for Auger ionization[29] and direct ionization.[30]

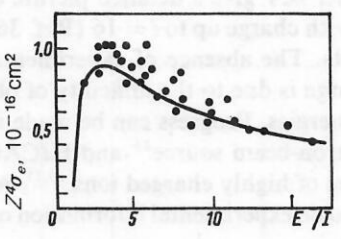

FIG. 1. Dependence of the ionization cross section for hydrogen-like ions on the electron energy in relative units: points—experimental data of Refs. 25 and 26; solid line—calculation of Ref. 27.

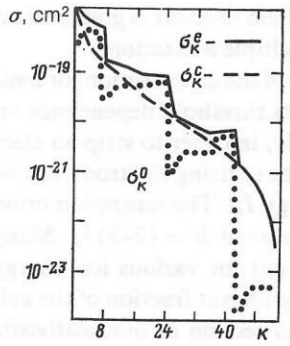

FIG. 2. Calculated cross sections for ionization of xenon ions by electrons of energy 20 MeV: points—Auger ionization cross section[29]; dashed line—direct ionization cross section[30]; solid line—total ionization cross section.

Ion–ion processes

The nature of the interaction of the ions with each other and with the neutral gas in the electron beam is determined by the ion kinetic energy. The ion transverse motion is oscillatory. The oscillation energy is determined by the depth of the potential well produced by the beam charge. The electric field potential U is proportional to the linear density of the electron beam N_e and, for example, when the charge density is uniform over the cross sectional area, $U = eN_e$ at the edge of the beam. When the relative velocities of the ion collisions are larger than the typical velocity v_0 of electrons in the outer shells (for the hydrogen atom $v_0 = 2.19 \cdot 10^8$ cm·sec^{-1}) the most probable process is the ionization of an ion with a smaller charge or ionization of a neutral atom. However, such ion velocities can occur in electron beams with linear density $N_e > 10^{13}$ cm^{-1}, which for relativistic electrons corresponds to currents of hundreds of kiloamperes.

The cross sections for the dominant processes in electron beams are given in Fig. 3 as functions of the energy of the interacting particles for the case of hydrogen atoms and ions.[32]

In a wide range of ion energies 1–10^4 eV·nucleon^{-1}, which corresponds to linear beam densities of 10^8–10^{12} cm^{-1}, the most probable reaction between ions is charge exchange, $A^{i+} B^{k+} \to A^{(i-1)+} + B^{(k+1)+}$. In this energy range the cross section for this process depends weakly on the collision velocity and reaches its maximum value. In the last 10–20 years ion charge exchange at low energies ($v < v_0$) has attracted a great deal of attention in connection with the development of plasma physics and the problem of controlled thermonuclear fusion. Several hundreds of experimental and theoretical studies have been published on this problem. The present situation is most fully described in reviews and conference proceedings.[33–35] The experimental data at ion energies of order keV give a detailed picture of charge exchange for ions with charge up to $i = 16$ (Ref. 36) and various neutral targets. The absence of experimental data on ions of higher charge is due to the difficulty of obtaining such ions at low energies. Progress can be made in this area by using an electron-beam source[25] and HICAC electron rings as the source of highly charged ions.[10,11] At the present time there is also no experimental information on ion–ion charge exchange.

The computation of the charge-exchange cross section is a complicated quantum-mechanical problem in which it is necessary to take into account the large number of possible excited states of the ion which gains an electron. The general form of the total cross section for charge exchange summed over all quantum states at collision energies corresponding to the maximum value can be represented by a simple empirical dependence:

$$\sigma_{ki} = Ai^{\alpha} I_k^{-\beta}. \tag{3}$$

Most theoretical calculations and analyses of the experimental data give the value $\alpha = 1$–1.2 (in several models $\sigma_{ki} \sim i \ln i$) and $\beta = 2$–3 (Refs. 33–35). As the collision energy increases the charge-exchange cross section decreases rapidly, while the parameter α grows. For example, $\alpha = 2$ for $v \sim v_0$, while $\sigma_{ki} \sim i^5/v^{12}$ for $v \gg v_0$ (Refs. 35 and 37). The magnitude of the charge exchange cross section varies from 10^{-15} cm^2 for charge exchange between singly charged ions and neutral atoms to 10^{-13} cm^2 for the process[38]

$$Xe^{54+} + H \to Xe^{53+} + H^+.$$

Ion storage in electron beams and rings

In the first studies of ion storage (Refs. 22, 28, 29, and 39–43) the calculations were carried out neglecting ion charge exchange. Ion storage in an electron beam taking into account single charge exchange is described by the following system of equations:

$$\left.\begin{aligned}
&\frac{dN_0}{dt} = \pi d\bar{u}\,(n - N_0/S) - \sigma_0^e N_0 v_e \rho_e - \sum_{k=1}^{Z} \sigma_{0k} v_{0k} N_0 N_k / S;\\
&\frac{dN_i}{dt} = (\sigma_{i-1}^e N_{i-1} - \sigma_i^e N_i)\, v_e \rho_e + \Big[\sum_{k=i}^{Z} \sigma_{i-1k} v_{i-1k} N_{i-1} N_k\\
&+ \sum_{k=0}^{i} \sigma_{ki+1} v_{ki+1} N_k N_{i+1} - \sum_{k=i+1}^{Z} \sigma_{ik} v_{ik} N_i N_k\\
&- \sum_{k=0}^{i-1} \sigma_{ki} v_{ki} N_k N_i\Big] \Big/ S;\\
&\frac{dN_Z}{dt} = \sigma_{Z-1}^e N_{Z-1} v_e \rho_e - \sum_{k=0}^{Z-1} \sigma_{kz} v_{kz} N_k N_z / S, \quad 1 \leqslant i < Z.
\end{aligned}\right\} \tag{4}$$

Here N_0 and N_i are the linear densities of neutral atoms and ions of charge i in the beam, n is the density of neutral atoms outside the beam, $\bar{u}$ is the average value of the component of the neutral velocity normal to the beam cross section, Z is the charge of the atomic nucleus, S and d are the beam cross-sectional area and diameter, v_{ik} is the average relative velocity of ions with charges i and k, and v_e and ρ_e are the velocity and density of the electrons in the beam.

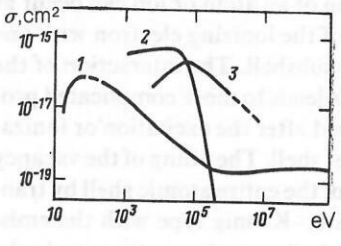

FIG. 3. Dependences of the cross sections for ionization by electron collisions (*1*), charge exchange (*2*), and ion collisions (*3*) on the particle energy E.

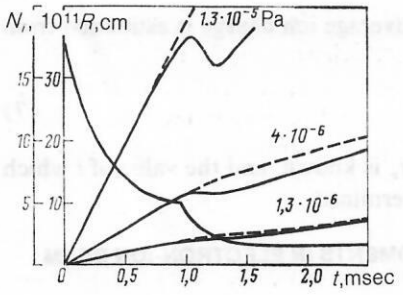

FIG. 4. Time dependence of the radius of the electron ring and the calculated number of nitrogen ions in it for various pressures of the residual gas in the accelerator chamber: solid line—calculation including charge-exchange processes; dashed line—neglecting charge-exchange processes.

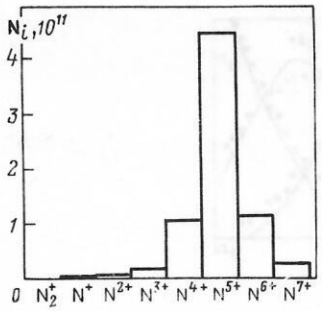

FIG. 5. Calculated distribution of the number of nitrogen ions in charge states at the end of the compression of the electron ring for number of electrons in the ring equal to 10^{13} and pressure of the residual gas in the accelerator chamber equal to $4 \cdot 10^{-6}$ Pa.

Multiple charge exchange and ionization processes can be taken into account by the inclusion of the corresponding terms in the right-hand side of the equations in the system (4).[44] In the case of storage of ions from a molecular gas, first molecular ions are produced and then they dissociate concurrently with the subsequent ionization.[21] These processes are important only at the earliest stage of the storage.

Let us calculate the storage of nitrogen ions from the residual gas in the accelerator chamber in the formation of an electron ring in the HICAC prototype.[44] In Fig. 4 we show the variation of the number of ions for different values of the residual-gas pressure and average radius of the electron ring. The calculations were carried out taking into account ion single and double charge exchange. The dashed lines correspond to the calculations neglecting ion–ion interactions. In Fig. 5 we show the charge distribution of the ions at the final stage of the storage.

The results of the calculations agree with measurements of the parameters of electron-ion rings and with experiments on ion acceleration in the HICAC prototype.

The number of ions in the ring can be determined experimentally according to the electron bremsstrahlung.[45–49] Bremsstrahlung arises because of the Coulomb interaction between the electrons and the nuclei of the ions and neutral atoms in the ring. The product $N_e(N_i + N_0)$ can be measured. The number of electrons in the ring is determined at the initial stage, when ions have not yet accumulated and only atoms of the residual gas, whose pressure is known, are present in the ring. When N_e is known, the number of accumulated ions can be found at the end of the confinement period.

The theory of the collective method of ion acceleration by electron rings imposes rigorous requirements on the electron ring parameters.[9,50] For the successful acceleration of ions it is necessary that the number of electrons and ions, the ion charge, and the ring dimensions lie within strictly defined limits. The characteristics of electron-ion rings measured in experiments on ion acceleration in the HICAC prototype[51–54] are in agreement with the calculated values.

The synchrotron radiation of relativistic electrons is also used for ring diagnostics. Of particular interest is the theoretically predicted and experimentally detected phenomenon of the broadening of the angular distribution of synchrotron radiation in an electron ring when ions are stored in it.[55,56]

The synchrotron radiation of a relativistic electron is concentrated in a small angular range $\Psi \sim 1/\gamma$ (γ is the relativistic factor) near the direction of the velocity. In the accelerator the electrons undergo betatron oscillations relative to the equilibrium orbit. This leads to oscillations of the electron velocity vector relative to the general direction of motion of the electron beam and to an increase of the width of the synchrotron radiation angular distribution. The half-width of the angular distribution of the radiation in the axial direction is[57]

$$\theta_{\text{rad}} = \sqrt{\Psi^2 + \theta_z^2},$$

where θ_z is the rms angular deviation of the particles from the median plane of the accelerator due to the betatron oscillations. The frequency of the betatron oscillations is determined by the external focusing and the proper charge of the ions in the beam. The angular distribution of the synchrotron radiation becomes broader as the number of ions increases. The number of ions in the electron ring of a collective accelerator is roughly proportional to the number of electrons.

The synchrotron radiation in the HICAC prototype has been measured as a function of the number of electrons in the ring. The results are shown in Fig. 6. Here the vertical axis corresponds to the half-width of the distribution of the intensity $\delta = L\theta_{\text{rad}}$, where $L = 75$ cm is the effective measurement base. The number of electrons in the ring N_e in relative units is plotted along the horizontal axis. In this figure the solid lines show the calculated dependences of δ on N_e found from the equations for the second moments of the electron and ion distribution functions. These equations are derived in Sec. 2. The calculations were carried out for two models of the ring confinement. In the first case (curve 1) the decrease of the cross sectional area of the electron ring due to ion

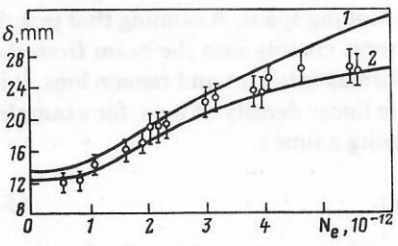

FIG. 6. Variation of the half-width of the intensity of synchrotron radiation as a function of the number of electrons in the ring: 1—calculation neglecting ion focusing of the electrons with initial cross-sectional radius of the ring equal to 1.7 cm; 2—including pion focusing and with the initial radius equal to 1.5 cm; points—experimental values.

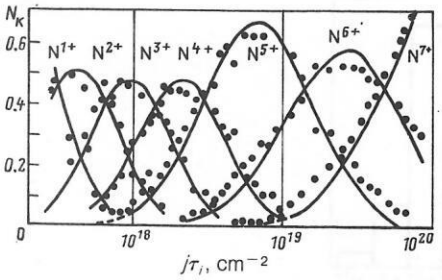

FIG. 7. Evolution of the charge distribution of nitrogen ions in an electron-beam ion source.

focusing was neglected and the initial radius of the ring cross section was taken to be $a_0 = 1.7$ cm. Curve 2 was obtained taking this decrease into account and using $a_0 = 1.5$ cm. For a small number of electrons $N_e \lesssim 10^{12}$, when the ion fields can be neglected, $\delta = L\Psi$. When the number of electrons is large, the effect of the ion proper charge on the strength of the focusing becomes important; the width of the angular distribution of the radiation is determined by the betatron oscillations and $\sigma = L\theta_z$.

Study of the dynamics of ion storage in electron beams and rings makes it possible not only to measure the parameters of the ion component, but also to determine the cross section for ion ionization by electron collisions. For this purpose a method was developed in Refs. 43 and 58 for solving the inverse ionization problem, and the ionization cross sections of all the ions of C, N, O, Ne, Ar, and also Kr (up to Kr^{33+}) and Xe (up to Xe^{47+}) were measured using the KRION-2 ion source.[59,60] In Fig. 1 we give the values of the ionization cross sections of hydrogen-like ions up to Ar^{17+} inclusive. The evolution of the charge distribution of nitrogen ions is shown in Fig. 7.[59] The solid lines correspond to the calculations, which made use of the ionization cross sections giving the best approximation to the experimental data.

As a rule, the calculation of ion storage taking into account all the charge states in electron beams and rings involves complicated computer calculations. However, in some special cases there are analytic solutions of the system of equations (4) (Refs. 39, 40, and 43) or approximate formulas for determining the total number of ions and their average charge.[61] It is simplest to determine the total number of ions in the beam. Here two limiting cases are possible. In dense electron beams the influx of neutral atoms from the outside does not manage to compensate for the decrease of neutral atoms due to ionization and charge exchange. As a result, the density of neutral gas in the beam is significantly lower than in the surrounding space. Assuming that practically all the neutral atoms coming into the beam from the residual gas are transformed into ions and remain ions, it is possible to estimate the linear density of ions, for example, nitrogen, produced during a time t:

$$N = \sqrt{\frac{2\pi}{3}}\, u_i\, dn_0 t. \tag{5}$$

In more rarefied beams, where $n_e \ll u_i/\sigma_0^e dv_e$, the density of neutral atoms in the beam practically coincides with n_0 and

$$N = \sigma_0^e v_e n_0 N_e t, \tag{6}$$

where σ_0^e is the ionization cross section of neutral atoms of the residual gas. The average ion charge is estimated from the relation

$$j\tau = \sum_{k=0}^{i} 1/\sigma_k^2. \tag{7}$$

The ionization factor j_τ is known, and the value of i which best satisfies (7) is determined.

2. THE METHOD OF MOMENTS IN ELECTRON-ION BEAM DYNAMICS

Equations (4) given in Sec. 1 make it possible to follow the ion transitions between different charge states and to take into account the various ion–electron and ion–ion collision processes. The effect of the electron spatial distribution and of different ion charge states on the ion storage process and also the effect of the ion and electron proper charge on the particle motion are described by the system of self-consistent Vlasov equations. The particle motion in the phase space of the coordinates $\mathbf{x}$ and momenta $\mathbf{p}$ is determined by the distribution function $f(\mathbf{x}, \mathbf{p}, t)$, which satisfies the kinetic equation[62]

$$\frac{df}{dt} = \frac{\partial f}{\partial t} + \mathbf{v}\frac{\partial f}{\partial \mathbf{x}} + e\left(\mathbf{E} + \frac{1}{c}(\mathbf{v}\times\mathbf{B})\right)\frac{\partial f}{\partial \mathbf{p}} = S, \tag{8}$$

where $\mathbf{v}$ is the particle velocity and S is the collision integral.

The electric field strength $\mathbf{E}$ and magnetic field $\mathbf{B}$ are found from Maxwell's equations

$$\text{rot } \mathbf{E} = -\frac{1}{c}\frac{\partial \mathbf{B}}{\partial t};\quad \text{div } \mathbf{B} = 0;$$

$$\text{rot } \mathbf{B} = \frac{1}{c}\frac{\partial \mathbf{E}}{\partial t} + \frac{4\pi}{c}\mathbf{j};\quad \text{div } \mathbf{E} = 4\pi\rho$$

with the appropriate initial and boundary conditions. The field sources (the charge density ρ and the current $\mathbf{j}$) are split into external sources and sources related to the beam particles, for which

$$\rho = e\int f d^3\mathbf{p},\quad \mathbf{j} = e\int \mathbf{v} f d^3\mathbf{p}.$$

In the case where there are several types of particle, instead of the single equation (8) we have a system of such equations. In the Vlasov equations[62] the collision integral S usually describes inelastic interactions. In the case where there is a system of equations (8) for several ion components and electrons the collision integral must include terms corresponding to inelastic processes, i.e., ionization and charge exchange. In most of the cases considered, all of the processes can be divided into fast and slow processes. The particle kinematics or motion and, in many cases, the variation of averaged quantities, i.e. the left-hand side of (8), can be related to the fast processes. Then, neglecting the right-hand side of (8), we obtain the Liouville equation:

$$\frac{df}{dt} = \frac{\partial f}{\partial t} + \frac{\partial \mathbf{x}}{\partial t}\frac{\partial f}{\partial \mathbf{x}} + \frac{\partial \mathbf{p}}{\partial t}\frac{\partial f}{\partial \mathbf{p}} = 0.$$

When studying slow processes related to collisions and transitions between charge states, the integration of Eqs. (8) over the entire phase space of the coordinates and velocities gives the system of equations (4).

The solution of the system of Vlasov equations involves great computational difficulties, so in practice one uses a small number of exactly solvable beam models[63,64] or various numerical methods of solving the equations by computer.[65,66] The method of moments represents one of the new approaches to the problem. The principal aim of the method of moments is to give a brief (compared to the Vlasov equa-

tions) description of the beam dynamics which still allows the fundamental physical regularities to be followed.

The distribution-function moments method

Of particular interest in the study of charged-particle beams are averaged characteristics of the beam such as the average velocity, the rms dimensions, the emittance, the temperature, and so on.

There are several models which can be used to trace the time variation of the envelope or rms dimensions for charged-particle beams in electromagnetic fields. The Vladimirskiĭ–Kapchinskiĭ model is widely used for monoenergetic beams of density which is uniform in an elliptical cross-sectional area and not coupled to the particle transverse motion. This model has been generalized to the case of arbitrary charge density in the cross section of a beam with elliptical symmetry.[67,68] Yarkovoĭ[69] has constructed a self-consistent model of a beam which takes into account the coupling of the transverse motion and the variation of the particle mass due to acceleration. The application of the distribution function moments method to problems in charged beam dynamics has made it possible to generalize all these models and to solve a number of new, important problems.

In Ref. 13 the moments of the distribution function in the entire set of phase-space coordinates were introduced in a class of distribution functions integrable with arbitrary power-law wake. We note that in gaseous (hydro) dynamics one usually deals with spatially unbounded distributions, so that only moments in the velocities are used.

Let us consider the first moments of the distribution function. The zero-order moment

$$N = \int f(Y, \tau)\, dY \tag{9}$$

is, by virtue of (8), an integral of the motion and equal to the total number of particles in the bunch if Y is a vector corresponding to the transverse phase-space coordinates and the beam is monoenergetic.

The first-order moments form the vector

$$\overline{Y} = \frac{1}{N} \int Y f(Y, \tau)\, dY, \tag{10}$$

where the spatial components of the vector $\overline{Y}$ specify the position of the center of mass and the velocity components specify the average velocities. In fields which are linear in the phase-space coordinates the first-order moments satisfy the equation

$$\frac{d\overline{Y}}{d\tau} = A\overline{Y}. \tag{11}$$

The second-order central moments can be written as a symmetric square matrix

$$M = \frac{1}{N} \int (Y - \overline{Y})(\widetilde{Y} - \widetilde{\overline{Y}})\, f(Y, \tau)\, dY. \tag{12}$$

The symbol $\sim$ stands for matrix transposition. The diagonal elements of the matrix M give the rms dimensions and rms dispersions of the particle beam velocity. Let the particles in a transverse cross section of the beam move in linear external fields. We write the equation for the transverse motion as

$$dx/d\tau = v, \quad dv/d\tau = b^{\text{ext}} x + av + F^s(x, \tau), \tag{13}$$

where x and v are two-dimensional coordinate and velocity vectors and $F^s(x, \tau)$ is a vector related to the electromagnetic field of the beam.

Differentiating (12) with respect to τ and using the equation of continuity in phase space, for the case of fields linear in the coordinates we obtain

$$dM/d\tau = AM + M\widetilde{A}. \tag{14}$$

Here A is a block matrix constructed from the matrices b^{ext} and a:

$$A = \begin{pmatrix} 0 & I \\ b^{\text{ext}} & a \end{pmatrix} I = \begin{pmatrix} 1 & 0 \\ 0 & 1 \end{pmatrix}. \tag{15}$$

We write the matrix of the second-order moments in the block form

$$M = \begin{pmatrix} M_{xx} & M_{xv} \\ \widetilde{M}_{xv} & M_{vv} \end{pmatrix}, \tag{16}$$

where each 2×2 matrix M_{xx} corresponds to the moments of the spatial coordinates: $M^{ij}_{xx} = \overline{x_i x_j}$, and so on.

The second-order moments satisfy the system of differential equations (14), which we rewrite as

$$\left.\begin{aligned} dM_{xx}/d\tau &= M_{xv} + \widetilde{M}_{xv}; \\ dM_{xv}/d\tau &= M_{vv} + M_{xx}\widetilde{b}^{\text{exp}} + M_{xv}\widetilde{a} + \widetilde{F}_{sx}; \\ dM_{vv}/d\tau &= b^{\text{ext}} M_{xv} + \widetilde{M}_{xv} b^{\text{exp}} + aM_{vv} + M_{vv}\widetilde{a} + F_{sv} + \widetilde{F}_{sv}. \end{aligned}\right\} \tag{17}$$

The second-order square matrices F_{sx} and F_x are defined in terms of the vector $F^s(x,t)$:

$$F^{ij}_{sx} = \overline{F^s_i x_j}, \; F^{ij}_{sv} = \overline{F^s_i v_j}. \tag{18}$$

The system (17) will be closed if the matrices F_{sx} and F_{sv} are expressed in terms of the second-order moments. Closure occurs automatically for linear forces and in the one-dimensional case.[1)] The nonlinearity of the forces intrinsic to the system leads to an infinite coupled system of equations for the moments. An effective linearization of the electromagnetic forces for a beam with elliptically symmetric charge density was carried out in Refs. 14, 67, and 68 using the condition that the rms deviation of the linear forces from the true forces is a minimum (see the Appendix). As a result, the force matrices have the form

$$F_{sx} = b^s M_{xx}, \quad F_{sv} = b^s M_{xv}, \tag{19}$$

where the matrix b^s is expressed in terms of the matrix M_{xx}:

$$b^s = \frac{N_e r_e M_{xx}^{-1/2}}{\beta^3 \gamma^3 \operatorname{Sp} M_{xx}^{1/2}} \begin{cases} 1\text{—linear geometry} \\ \omega_0^2 R_0^2\text{—circular beam} \end{cases} \tag{20}$$

where $\beta = v_e/c$, ω_0 is the orbiting frequency, and γ is the relativistic factor of the electron.

The equations (19) imply that the electromagnetic force intrinsic to the system is replaced by an effective linear force:

$$F^s(x, \tau) = b^s x. \tag{21}$$

The problem of reconstructing the nonlinear electric field from the first moments of the charge density has been solved for a lepton beam and for a charged cylinder with circular cross section in Ref. 71. After substitution of (19) and (20) into (17) we obtain a system of nonlinear ordinary equations for the rms beam parameters. For a beam with circular cross section this system leads to the following equation for the rms beam radius R;

$$\frac{d^2R}{dt^2}+(\omega^2+\omega_L^2)\,R-\frac{2N_e r_e c^2}{\gamma^3 R}-\frac{E_1^2}{R^3}=0, \qquad (22)$$

where ω^2 is the square of the frequency related to the external focusing (for example, ion focusing in the case of electrons) and ω_L is the Larmor frequency.

The constant E_1 is determined from the relations[14]

$$E_1=4\,[\overline{(x_1-\bar{x}_1)^2}\,\overline{(v_1-\bar{v}_1)^2}-\overline{((x_1-\bar{x}_1)\,(v_1-\bar{v}_1))^2}-((x_1-\bar{x}_1)\times(v_2-\bar{v}_2))^2]\,|_{t=0}+M_3^2, \qquad (23)$$

where $M_3=J+2\omega_L R^2=\text{const}$ is the generalized azimuthal angular momentum (Busch's theorem) and J is the average value of the azimuthal canonical angular momentum. Equation (22) has been obtained by Lee and Cooper in Ref. 72. The propagation of an electron beam in a longitudinal magnetic field taking into account the space charge of the accumulated ions is described by the equation

$$\frac{d^2R}{dt^2}+\omega_L^2 R-\frac{2N_e r_e c^2}{\gamma R}\left(\frac{1}{\gamma^2}-f\right)-\frac{E_1^2}{R^3}=0, \qquad (24)$$

where f is the beam neutralization factor, equal to the ratio of the linear charge densities of the ions and electrons. When the Coulomb repulsion of the electrons is balanced such that $f>1/\gamma^2$, then according to (24) the beam is self-focused by magnetic constriction forces, and transport of the beam without a magnetic field becomes possible. The moments method is applicable to a wide variety of problems involving the transport and formation channels and the focusing structures in the acceleration of charged-particle beams. In Ref. 73 computational techniques were developed on the basis of the moments method and programs were written for analyzing periodic (or quasiperiodic) focusing structures in linear accelerators, beam transport channels, and bunchers taking into account space charge effects. For the beam at the meson factory of the Institute of Nuclear Research[74] (injection current equal to 140 mA) the moments method was used to calculate two variants of the injection channel.[75,76] Owing to the large savings of time, the moments method made it possible to optimize the channel.

Second-order moments for circular beams

Two models are generally used for studying the equilibrium characteristics of circular charged-particle beams and their behavior under adiabatic variation of the parameters of the external electromagnetic field. In the first model[77] the energy spread is not taken into account and the radial dimension of the beam is determined by the amplitudes of the particle betatron oscillations. In the second model[78] the radial phase space is assumed to be zero and the size is determined by the energy spread of the particles in the beam. Here we shall use the method of total moments of the distribution function to study the stationary states, free oscillations, and adiabatic variation of the rms dimensions of circular charged-particle beams with nonzero energy spread and radial phase space.[79]

We consider an azimuthally symmetric ring of charged particles having an energy spread and moving in a magnetic field $\mathbf{B}=(B_r, 0, B_z)$.

When a relativistic electron ring is contained for a long time, effects related to energy losses to synchrotron radiation and also electron scattering on the residual gas or the accumulated ions become important. The effect of radiation on the formation of electron rings has been studied in Ref. 80. The linearized equations of motion in cylindrical coordinates (R, θ, z) can be written as

$$\left.\begin{aligned}
&\ddot{x}+\left(\frac{\dot{\gamma}}{\gamma}+\frac{P}{\gamma mc^2}\right)\dot{x}+\omega_r^2 x+F_x+\delta F_x=\frac{\omega_0 M}{\gamma m R_0};\\
&\ddot{z}+\left(\frac{\dot{\gamma}}{\gamma}+\frac{P}{\gamma mc^2}\right)\dot{z}+\omega_z^2 z+F_z+\delta F_z=0;\\
&\dot{W}+P\left((1-2n)\frac{x}{c}+\frac{2W}{\gamma mc^2}\right)=0,
\end{aligned}\right\} \qquad (25)$$

where n is the magnetic field exponent, $x=R-R_0$, $W=M_\theta-M_\theta^0$, $\omega_{r,z}=\nu_{r,z}\omega_0$ is the betatron oscillation frequency, M_θ^0 is the generalized angular momentum and $P=2e^4B_z^2\gamma^2/(3m^2c^3)$ is the power corresponding to radiation losses of an equilibrium particle. The force $\mathbf{F}$ arises from the intrinsic electromagnetic field of the beam. The random force $\delta\mathbf{F}$ is related to electron scattering on ions and neutral atoms.[72] To make the system (25) complete, it is necessary to include the equation describing the variation of the large radius of the ring and the coupling of the electron energy to the magnetic field:

$$\left.\begin{aligned}
&\dot{R}_0+\frac{R_0}{(1-n)\,B_z}\left(\dot{B}_z-\frac{\dot{\bar{B}}_z}{2}\right)+\frac{R_0 P}{(1-n)\,\gamma mc^2}=0;\\
&\gamma mc^2=-cB_z R_0.
\end{aligned}\right\} \qquad (26)$$

Here B_z is the average value of the field B_z over the circle of radius R_0.

We form a column vector Y from the particle coordinates and velocities and, as usual, write the equation of motion (25) in the matrix form

$$dY/dt=AY+F+\delta F. \qquad (27)$$

The matrix A is defined as

$$\left.\begin{aligned}
&A=\begin{pmatrix}0 & \Sigma\\ b & a\end{pmatrix},\\
&\Sigma=\begin{pmatrix}1&0&0\\0&1&0\end{pmatrix},\quad b=\begin{pmatrix}-\omega_r^2 & 0\\ 0 & -\omega_z^2\\ -\frac{(1-2n)\,P}{c} & 0\end{pmatrix},\\
&a=\begin{pmatrix}-\frac{P}{\gamma mc^2}-\frac{\dot{\gamma}}{\gamma} & 0 & \frac{\omega_0}{\gamma m R_0}\\ 0 & -\frac{P}{\gamma mc^2}-\frac{\dot{\gamma}}{\gamma} & 0\\ 0 & 0 & -\frac{2P}{\gamma mc^2}\end{pmatrix}.
\end{aligned}\right\} \qquad (28)$$

The column vector F is constructed from the components of the Lorentz force related to the intrinsic electromagnetic field of the beam.

The matrices M_{xx}, M_{xv}, and M_{vv} are defined as before; for example, M_{xx} is the matrix of the rms beam dimensions:

$$M_{xx}^{ij}=\overline{x_i x_j},\ i,\ j=1,2. \qquad (29)$$

In contrast to (12), these matrices have different dimensions: M_{xx} and M_{vv} are symmetric square matrices of rank 2 and 3, respectively, and M_{xv} is a 2×3 matrix.

The second-order moments satisfy the system of differential equations

$$dM/dt=AM+M\tilde{A}+\overline{F\tilde{Y}}+\overline{Y\tilde{E}}+\overline{\delta F\tilde{Y}}+\overline{Y\delta\tilde{F}}. \qquad (30)$$

When the radial and the axial motion are separated, it is possible to find a particular solution of the system (30) with a diagonal matrix M_{xx}. For the second-order moments we have

$$\dot{\overline{x^2}} = 2\overline{xv_r};$$

$$\dot{\overline{v_r^2}} = -2\omega_r^2\overline{xv_r} - 2\left(\frac{P}{\gamma mc^2} + \frac{\dot{\gamma}}{\gamma}\right)\overline{v_r^2} + \frac{2c}{\gamma mR_0^2}\overline{Wv_r} + 2S_r;$$

$$\dot{\overline{xv_r}} = \overline{v_r^2} - \overline{x^2}\omega_r^2 - \left(\frac{P}{\gamma mc^2} + \frac{\dot{\gamma}}{\gamma}\right)\overline{xv_r} + \frac{c}{\gamma mR_0^2}\overline{Wx};$$

$$\dot{\overline{xW}} = \overline{v_rW} - \frac{(1-2n)}{c}P\overline{x^2} - \frac{2P}{\gamma mc^2}\overline{xW};$$

$$\dot{\overline{v_rW}} = -\omega_r^2\overline{xv_r} - \left(\frac{P}{\gamma mc^2} + \frac{\dot{\gamma}}{\gamma}\right)\overline{v_rW} + \frac{c\overline{W^2}}{\gamma mR_0^2} - \frac{(1-2n)}{c}P\overline{xv_r} - \frac{2P}{\gamma mc^2}\overline{v_rW}; \tag{31}$$

$$\dot{\overline{W}}^2 = \frac{-2(1-2n)}{c}P\overline{xW} - \frac{4P}{\gamma mc^2}\overline{W}^2;$$

$$\dot{\overline{z^2}} = 2\overline{v_zz};$$

$$\dot{\overline{zv_z}} = \overline{v_z^2} - \omega_z^2\overline{z^2};$$

$$\dot{\overline{v_z^2}} = -2\omega_z^2\overline{zv_z} + 2S_z,$$

where

$$S_{r,z} = \frac{1}{\gamma m}\int\int \gamma\delta F_{r,z}v_{r,z}f_if_e\,dY_i\,dY_e. \tag{32}$$

Here f_i, f_e, dY_i, and dY_e are the distribution functions and phase space elements of the ions and electrons, respectively. Using the results of Ref. 72 for arbitrary electron and ion densities in a small cross section of the ring, $\rho_e(x_e, z_e)$ and $\rho_i(x_i, z_i)$ we obtain the following for the rms variation of the transverse component of the electron velocity induced by scattering on charges I, for example, in the direction r (Ref. 79):

$$S_r = \frac{2I^2r_e^2c^3}{\gamma^2N}\int\int \frac{(x_i-x_e)^2\rho_e\rho_i}{[(x_i-x_e)^2+(z_i-z_e)^2]^2}\,dx_e\,dx_i\,dz_e\,dz_i. \tag{33}$$

The quantity S_z is given by a similar expression.

In the calculation of scattering on ions of charge i the integration in (33) runs over two regions of space: the first corresponds to scattering on a nucleus of charge Z and the $(Z-i)$ electrons of the ion with impact parameter smaller than the ion radius; the second corresponds to scattering on the ion as a whole with impact parameter larger than the ion radius but smaller than the beam diameter. We easily find the following for the case of equal electron and ion densities:

$$S_r = S_z = \frac{r_e^2N_ic^3}{2\pi ab\gamma^2}\left[(Z^2-Z-i)\ln\left(\frac{a_0\gamma mc}{\hbar(Z-i)^{1/3}}\right) + i^2\ln\left(\sqrt{\frac{2}{a^2+b^2}}\frac{ab}{a_0}\right)\right], \tag{34}$$

where a_0 is the Bohr radius, $\hbar$ is Planck's constant, a and b are the rms radii of the beam, $a = \sqrt{\overline{x^2}}$ and $b = \sqrt{\overline{z^2}}$, and $v_r = \sqrt{\overline{v_r^2}}$ and $v_z = \sqrt{\overline{v_z^2}}$.

The inclusion of the intrinsic fields leads to the usual Coulomb frequency shift

$$\nu_r^2 = 1 - n - \frac{r_eN_eR_0^2}{\gamma^3\beta^2a(a+b)}. \tag{35}$$

The system (31) fully describes the variation of the small dimensions of the ring and the spread in the angular momenta of an azimuthally symmetric beam taking into account radiation effects and the increase of the phase space due to electron scattering on the stored ions.

When the parameters of the system (31) depend weakly on the time, so that

$$\frac{\gamma}{\omega_0\gamma} \sim \frac{\dot{R}_0}{\omega_0R_0} \sim \varepsilon \ll 1, \tag{36}$$

the first derivatives with respect to time in (31) are quantities of order ε. Neglecting smaller terms, we obtain

$$\frac{d}{dt}\left(\frac{\gamma v_r^2}{\omega_r}\right) = \frac{\gamma}{\omega_r}\left[\frac{Pv_r^2}{\gamma mc^2}\left(\frac{(1-2n)c^2}{R_0^2\omega_r^2} - 1\right) + S_r\right]; \tag{37}$$

$$\frac{d}{dt}\left(\frac{\gamma v_z^2}{\omega_z}\right) = \frac{\gamma}{\omega_z}\left(S_z - \frac{Pv_z^2}{\gamma mc^2}\right); \tag{38}$$

$$\frac{d\overline{W}^2}{dt} = -\frac{2P\overline{W}^2}{\gamma mc^2}\left(\frac{(1-2n)c^2}{R_0^2\omega_r^2} + 2\right), \tag{39}$$

where the rms velocities are

$$v_r^2 = a^2\omega_r^2 - \frac{c\overline{W}^2}{\gamma^2m^2R_0^4\omega_r^2};\quad v_z^2 = b^2\omega_z^2. \tag{40}$$

When the effects of synchrotron radiation and electron scattering are insignificant, Eqs. (37)–(39) give the familiar adiabatic invariants[79]:

$$\left.\begin{aligned}&\gamma\omega_r\left(a^2 - \frac{c\overline{W}^2}{\gamma^2m^2R_0^4\omega_r^4}\right) = E_r = \text{const};\\ &\gamma\omega_zb^2 = E_z = \text{const};\quad \overline{W}^2 = \text{const},\end{aligned}\right\} \tag{41}$$

where E_r and E_z correspond to the effective phase space of the transverse motion of the particles in the beam.

The first equation in (41) is conveniently rewritten using the "betatron" and "synchrotron" dimensions $a^2 = a_s^2 + a_b^2$, where $a_b^2 = E_r/\gamma\omega_r$ and $a_s^2 = c^2\overline{W}^2/\gamma^2m^2R_0^4\omega_r^4$. For $a_s \ll a_b$, (41) leads to the results of the model of Ref. 77; in the opposite case we obtain the equations found in Ref. 78. Neglecting the contribution from the intrinsic fields, from (39) we find[80]

$$\frac{d\overline{W}^2}{dt} = 2\left(\frac{3-4n}{1-n}\right)\overline{W}^2. \tag{42}$$

Estimates indicate that for typical values of the parameters of electron rings in collective accelerators the characteristic times of processes with synchrotron radiation[10] and electron scattering on the accumulated ions[81] are of order 10–100 msec. For the long electron-ring confinement time needed, for example, to obtain highly charged ions in collective accelerators, synchrotron radiation causes the transverse dimensions of the ring to decrease and for $0 \leqslant n \leqslant 3/4$ leads to a spread in the electron generalized angular momentum, while electron scattering on ions tends to increase the small dimensions of the beam. The passage of a linear electron beam through a gas or through solid films also leads to an increase of the transverse dimensions of the beam, which can be taken into account in Eq. (22). The experiments carried out by Briggs *et al.*[82] on beam propagation in a gas have shown that there is good agreement between the measured values of the rms radius and those calculated using the moments method.[83]

In the passage of an electron beam through thin solid films, when the variation of the beam energy and transverse dimensions can be neglected, the final rms emittance of the beam is given by $\varepsilon = \sqrt{\varepsilon_0^2 + \Delta\varepsilon^2}$, where $\varepsilon_0 = av/v_e$ is the initial emittance. The increment is

$$\Delta\varepsilon^2 = \frac{4\pi a^2r_e^2n_0c^4Z^2d}{v_e^4\gamma^2}\ln\frac{137}{Z^{1/3}}, \tag{43}$$

where n_0 is the number of atoms with nuclear charge Z per unit volume of the film and d is the film thickness.[84] In Fig. 8 we show the calculated values of the relative increase of the emittance $\varepsilon/\varepsilon_0$ for a beam with parameters $a = 1$ cm and $\gamma = 4.3$ passed through a titanium foil (curve 1) and a lav-

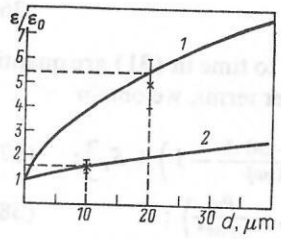

FIG. 8. Relative variation of the electron-beam emittance as a function of the thickness of a titanium (curve 1) and a lavsan (curve 2) film in the passage of the beam through the film. The points are the experimental values.

san film (curve 2) as a function of the film thickness, together with the experimentally measured emittances, which, as seen from the figure, are in satisfactory agreement with the calculated values.

Multicomponent charged beams

The moments method can be used to model the storage and subsequent ionization of ions in electron beams, to trace the variation of the dimensions of each charge component, and to take into account the effect of the different charge states on each other. The equations of motion of electrons and ions of charge state i are written as[85,86]

$$\begin{aligned}
&\ddot{x}_e+\frac{\dot{\gamma}}{\gamma}\dot{x}_e+\omega_x^2 x_e-\frac{1}{m\gamma}\left(F_x^{ee}+\sum_{i=1}^{z}F_x^{ei}\right)=0;\\
&\ddot{z}_e+\frac{\dot{\gamma}}{\gamma}z_e+\omega_z^2 z_e-\frac{1}{m\gamma}\left(F_z^{ee}+\sum_{i=1}^{z}F_z^{ei}\right)=0;\\
&\ddot{x}_i-\frac{1}{AM}\left(F_x^{ie}+\sum_{j=1}^{z}F_x^{ij}\right)=0;\\
&\ddot{z}_i-\frac{1}{AM}\left(F_z^{ie}+\sum_{j=1}^{z}F_z^{ij}\right)=0,\ i,\ j=1,\ 2,\ 3\ \ldots,\ Z.
\end{aligned}\tag{44}$$

Here, as before, the index e means that the quantity in question refers to electrons, while i and j refer to one of the z ionic charge states; x is the deviation of the particle radius from the equilibrium value. For circular beams $\omega_x^2=(1-n)c^2/R_0^2$ and $\omega_z^2=nc^2/R_0^2$. The forces F^{ei}, F^{ie}, F^{ee}, and F^{ij} are related to the proper change of the components in the ring; for example, F^{ei} is the force acting on an electron due to ions of charge state i. The ion distribution function including ion–ion charge exchange satisfies the following chain of kinetic equations:

$$\begin{aligned}
\frac{df_i}{dt}=&\rho_e c\,(\sigma_{i-1}^e f_{i-1}-\sigma_i^e f_i)\\
&+\sum_{j=0}^{z}\Big(\int f_{i+1}f_j\sigma_{i+1,j}|\mathbf{v}_{i+1}-\mathbf{v}_j|\,dv_{xj}\,dv_{zj}\\
&+\int f_j f_{i-1}\sigma_{ji-1}|\mathbf{v}_j-\mathbf{v}_{i-1}|\,dv_{xj}\,dv_{zj}\\
&-\int f_i f_j|\mathbf{v}_i-\mathbf{v}_j|\,(\sigma_{ij}+\sigma_{ji})\,dv_{xj}\,dv_{zj}\Big),
\end{aligned}\tag{45}$$

where σ_i^e is the cross section for electron ionization of an ion of charge i with $\sigma_z^e=0$, σ_{ij} is the cross section for charge exchange $A^{i+}+B^{i+}\to A^{(i-1)+}+B^{(j+1)+}$, and f_0 is the neutral-atom distribution function.

Following Refs. 85 and 86 we write the equations for the rms dimensions as

$$\begin{aligned}
&\ddot{a}_e+\frac{\dot{\gamma}}{\gamma}\dot{a}_e+\omega_{xe}^2 a_e-\frac{E_{xe}^2}{\gamma^2 a_e^2}=0;\\
&\ddot{b}_e+\frac{\dot{\gamma}}{\gamma}\dot{b}_e+\omega_{ze}^2 b_e-\frac{E_{ze}^2}{\gamma^2 b_e^2}=0;\\
&\ddot{a}_i+\omega_{xi}^2 a_i-\frac{E_{xi}^2}{a_i^2}=0;\\
&\ddot{b}_i+\omega_{zi}^2 b_i-\frac{E_{zi}^2}{b_i^2}=0,
\end{aligned}\tag{46}$$

where ω is the average frequency of the proper oscillations of the given type of particle and E is the effective phase space of the electron and ion components.

When the ion accumulation occurs slowly compared to the particle proper oscillation periods, the effective phase spaces remain constant. In the case of circular beams with rms deviation of the electron generalized momentum $\overline{W^2}$ the system (46) becomes a system of algebraic equations analogous to (41):

$$\left.\begin{aligned}
&\gamma\omega_{xe}\left(a_e^2-\frac{\overline{W}^2c^2}{\gamma^2m^2\omega_{xe}^4R^4}\right)=E_{xe};\ \gamma\omega_{ze}b_e^2=E_{ze};\\
&\omega_{xi}a_i^2=E_{xi};\ \omega_{zi}b_i^2=E_{zi},\ i=1,\ 2,\ 3,\ \ldots,\ Z.
\end{aligned}\right\}\tag{47}$$

If it is assumed that the electron and ion densities obey Gaussian distributions over the beam cross section,

$$\rho_{e,i}=\frac{N_{e,i}}{2\pi a_{e,i}b_{e,i}}\exp\left(-\frac{x^2}{2a_{e,i}^2}-\frac{z^2}{2b_{e,i}^2}\right),\tag{48}$$

where N_{ei} are the particle linear densities, the oscillation frequencies are[86]

$$\begin{aligned}
\omega_{xe}^2=&\frac{c^2}{R_0^2}(1-n)-\frac{e^2N_e}{\gamma^3ma_e(a_e+b_e)}\\
&+\frac{2e^2}{\gamma m}\sum_{i=1}^{z}\frac{iN_i}{(a_e^2+a_i^2+\sqrt{(a_e^2+a_i^2)(b_e^2+b_i^2)})};\\
\omega_{ze}^2=&\frac{nc^2}{R_0^2}-\frac{e^2N_e}{\gamma^3mb_e(a_e+b_e)}\\
&+\frac{2e^2}{\gamma m}\sum_{i=1}^{z}\frac{iN_i}{(b_e^2+b_i^2+\sqrt{(a_e^2+a_i^2)(b_e^2+b_i^2)})};\\
\omega_{xi}^2=&\frac{2ie^2}{AM}\left(\frac{N_e}{a_e^2+a_i^2+\sqrt{(a_e^2+a_i^2)(b_e^2+b_i^2)}}\right.\\
&\left.-\sum_{j=1}^{z}\frac{jN_j}{a_i^2+a_j^2+\sqrt{(a_i^2+a_j^2)(b_i^2+b_j^2)}}\right);\\
\omega_{zi}^2=&\frac{2ie^2}{AM}\left(\frac{N_e}{b_e^2+b_i^2+\sqrt{(a_e^2+a_i^2)(b_e^2+b_i^2)}}\right.\\
&\left.-\sum_{j=1}^{z}\frac{jN_j}{b_i^2+b_j^2+\sqrt{(a_i^2+a_j^2)(b_i^2+b_j^2)}}\right).
\end{aligned}\tag{49}$$

Neglecting the terms in Eq. (45) related to charge exchange, for the density (48) we obtain

$$dN_i/dt=\rho_e c\,(\sigma_{i-1}N_{i-1}-\sigma_i N_i).\tag{50}$$

Equations (47) and (50) together with (49) have been used to calculate the adiabatic contraction of the electron ring in the adhesator of the adiabatic generator of charged toroids in the HICAC prototype in an atmosphere of residual gas (nitrogen).[86]

The time dependences of the radius R, the relativistic factor γ, and the exponent of the falloff of the external magnetic field n were approximated by analytic functions of the time.

The electron ring parameters are close to the ring pa-

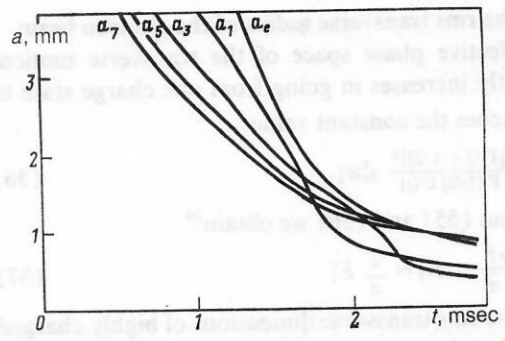

FIG. 9. Variation of the rms dimensions of the electron (a_e) and ion (a_1–a_7) components at the final stage of compression of an electron ring.

rameters for the HICAC adhesator[9]: the initial radius is $R_0 = 35$ cm, the dimensions of the ring cross section are $a_e = b_e = 2$ cm, and the number of electrons in the ring is $N_e = 10^{13}$. It was assumed that the "synchrotron" a_s and "betatron" a_b radial dimensions of the cross sections coincide at the instant of injection. In this variant of the calculation the pressure of the residual gas in the adhesator chamber was $4 \cdot 10^{-6}$ Pa (3.10^{-8} mm Hg). During the ring contraction time (about 2.3 msec) the average ion charge state increases to $i = 5$ and the neutralization of the electron charge reaches 40%–50%. The dispersion of the ion distribution in the charge state is 0.6.

In Fig. 9 we show the time dependences of the rms dimensions of the cross section of an electron-ion ring $a_{e,i}$ during the final stage of the contraction. The axial dimensions of the ring $b_{e,i}$ roughly coincide with the radial dimensions. The curves show that at the end of the contraction the rms ion dimensions a_5 coincide with the electron dimensions. This is mainly due to the decrease of the ion oscillation frequencies as a result of neutralization of the electron charge.

3. OBTAINING HIGHLY CHARGED IONS IN ELECTRON-ION BEAMS

Problems in obtaining highly charged ions

The production of beams of highly charged ions, including ions completely stripped of electron shells, is of great importance at the present time. The larger the ratio of the ion charge i to the ion mass number A, the more effective is the accelerator operation. Highly charged ions are needed for spectroscopic research and for measurements of the ionization and charge-exchange cross section. Study of α and β decays of nuclei in the absence of electron shells is of great interest.

Ions of very high charge and nuclei of all the gaseous elements through krypton have been obtained using the KRION-2 ion source.[2] Nuclei of heavier elements are obtained by stripping low-charge ions, which have been accelerated to energies of order 10 MeV/nucleon and above, in a gaseous or solid target (a stripper). Accelerated beams of highly charged ions are used in nuclear-physics research or for further acceleration. Highly charged ions of low energy are used in many areas of research and applied problems. There are several factors which limit the possibilities of obtaining highly charged ions in electron beams and rings in addition to the technical difficulties due to the long containment time. Some of the most important are:

(a) charge exchange on the residual gas in the accelerator chamber;

(b) neutralization of the proper charge of the beam by ions produced from the residual gas;

(c) ion losses due to heating by the beam electrons.

We shall discuss these problems in detail.

a. The average ion charge is increased by ionization by electron collisions. As the ion charge i increases the ionization cross section σ_i^e decreases and the process slows down. Meanwhile, the cross section for ion charge exchange on neutral atoms σ_{i0} is increased roughly in proportion to the charge i and can reach values of 10^{-13} cm^2 (Refs. 38 and 88). The density of residual-gas atoms n_0 needed to obtain ions in charge state i in a beam with electron density n_e can be determined from the condition[89]

$$\frac{n_0 \sigma_{i0} v_i}{n_e \sigma_i^e v_e} \ll 1, \tag{51}$$

where v_i and v_e are the ion and electron velocities, respectively.

b. In electron beams and rings ions are confined in the potential well of the electron proper charge. Ions produced from the residual gas neutralize the electron charge and decrease the well depth. The number of ions in the beam and the corresponding requirement on the residual-gas pressure are determined by (5) or (6) as functions of the electron density of the beam and the neutral-gas ionization cross section. The cases where ion production occurs only at the edge of the beam and where the production is uniform over the entire cross section of the beam have been studied in Ref. 90.

c. Owing to elastic collisions with electrons, the ion oscillation energy gradually increases and can exceed the depth of the beam potential well. This results in a loss of ions. The increase of the energy of ions with charge $i \approx Z$ is given by an expression similar to the collision integral (34):

$$\frac{d\varepsilon_i}{dt} = \frac{r_e^2 Z^2 N_e m^2 c^3}{a_e^2 \beta A M} \ln\left(\frac{2\gamma\beta a_e}{137\, r_e}\right), \tag{52}$$

where $\beta = v_e/c$.

Ion storage in electron beams of long duration

We shall consider electron beams whose duration is significantly larger than the characteristic times for ion production and accumulation, i.e., 1 msec to 1 sec and greater. The currents in such beams do not exceed several amperes, and the electron energy is tens to hundreds of keV. The most typical examples are the electron beams of electron-beam ion sources.

At the present time electron-beam sources are being developed and used for heavy-ion accelerators at several scientific centers.[91–94] The KRION-1 source has been used since 1977 at Dubna to accelerate C, N, 0, and Ne nuclei at the synchrophasotron.[95] The KRION-2 source has been used to obtain ions of record charge states which are used in spectroscopic research, for measuring ionization cross sections, and in other experiments.[25]

The electron-beam source EBIS is an electron accelerator with a drift tube. The electron beam is strongly focused by a longitudinal magnetic field. The construction and operation of the KRION-2 ionizer are shown in Fig. 10 (Ref. 87). The cryomagnetic system of the KRION-2 ionizer ensures that the field focusing the electron beam, $B = 2.25$ T, is maximal over the ionizer length 1.2 m. The cathode of the

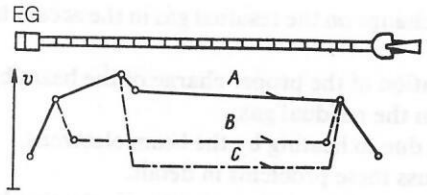

FIG. 10. Schematic depiction of the electronic–optical system and distribution of the electric potential U along the drift structure of the KRION ionizer: A—extraction of the ions from the ionizer; B—injection of ions of the working substance; C—containment and ionization.

electron gun of diameter 0.8 mm is located in the increasing magnetic field of a solenoid with $B = B_{max}/6$, which ensures that the electron beam is compressed to the equilibrium radius $a = 0.15$ mm. The drift structure consists of 25 isolated sections. The working gas from which the ions are produced flows into the third section. The temperature in the drift tube is maintained at 4.2 °K during the operation, which ensures that the residual-gas pressure is less than 10^{-10} Pa (10^{-12} mm Hg). The pulsed injection of ions of the working substance into the electron beam, and the extraction of the ions from the beam in the longitudinal direction are accomplished by systematically changing the distribution of the potential U along the ionizer axis: $B \to C \to A$. The construction, operation, and results of experimental studies of the storage of highly charged ions are given in the reviews of Refs. 7 and 25. The limiting parameters obtained in the KRION-2 ionizer are as follows: electron energy up to 22 keV, current density j up to $4.2 \cdot 10^{21}$ cm$^{-2}\cdot$sec^{-1} (650 A/cm^2), ionization time up to 5.5 sec, and ionization factor $j\tau$ up to $8 \cdot 10^{21}$ cm^{-2}.

The construction of the cathode and a strong longitudinal magnetic field ensure that the electron density is uniform over the cross section of the beam. Ion storage in electron beams with constant density has been studied in Refs. 9, 90, and 96–98. In uniformly charged electron beams ions are produced at any point of the cross section with equal probability. If their initial thermal velocities are neglected, the distribution function of singly charged ions is[9]

$$f_1 = \frac{N_1 AM}{4\pi^2 a_1^2 \omega^1}\,\sigma(\varepsilon_b - \varepsilon)\,\delta(M_\varphi), \tag{53}$$

where M_φ is the ion angular momentum, ε is the ion energy $\varepsilon_b = N_e r_e mc^2$ is the ion energy at the edge of the beam, $\omega_1 = (N_e r_e mc^2/(2AMa_e^2))^{1/2}$ is the oscillation frequency of singly charged ions, A is the ion atomic number, and M is the nucleon mass. The distribution function (53) corresponds to the ion density in a transverse cross section of the beam[96,97]

$$\rho_1 = \frac{N_1}{2\pi^2 a^2}\,\frac{\sqrt{a^2 - r^2}}{r}, \tag{54}$$

rms radius $a_1 = a/2\sqrt{2}$, and rms velocity of the transverse oscillations $v_i^2 = a_e^2\omega_1^2$.

The density (54) has an unphysical singularity at the center of the beam owing to the fact that in the derivation we have neglected the velocities of the neutral atoms. In electron beams whose dimensions are maintained by stationary external electromagnetic fields, the rms dimensions of ionic charge states decrease with increasing charge i according to the law[96–98]

$$a_i^2 = a_1^2\,\frac{2\Gamma(i+1/2)}{\Gamma(1/2)\,\Gamma(i+1)}, \quad a_1^2 = a_e^2/2. \tag{55}$$

Here a_e is the rms transverse radius of the electron beam.

The effective phase space of the transverse motion, which slightly increases in going from one charge state to another, reaches the constant value

$$E_i^2 = 4\,\frac{[\Gamma(i+1/2)]^2}{\Gamma(1/2)\,\Gamma(i)}\,a_e^2\omega_1^2. \tag{56}$$

For $i \gg 1$, from (55) and (56) we obtain[99]

$$a_i^2 = \frac{2a_1^2}{\sqrt{\pi i}}; \quad E_i^2 = \frac{4}{\pi}\,E_1^2. \tag{57}$$

Therefore, the rms transverse dimensions of highly charged ions can be 3–4 times smaller than the dimensions of a uniformly charged electron beam. The average total energy of the ion transverse oscillations is defined as

$$\varepsilon_i = 2AMa_i^2\omega_i^2 = \sqrt{\frac{i}{\pi}}\,N_e r_e mc^2. \tag{58}$$

The expression (52) can be used to find the rate of the relative increase of the ion energy for $i \approx Z$ due to collisions with the beam electrons:

$$\frac{1}{\varepsilon_i}\frac{d\varepsilon_i}{dt} = \sqrt{\pi Z}\,\frac{Z}{A}\,\frac{m}{M}\,\frac{r_e c}{a_e^2}\,\ln\left(\frac{2\gamma\beta a_e}{137\,r_e}\right). \tag{59}$$

For heavy ions $Z/A \approx 0.4$. Using the parameters of the electron beam of the KRION-2 ionizer,[87] for electron energy equal to 10 keV we obtain

$$\frac{1}{\varepsilon_i}\frac{d\varepsilon_i}{dt} \approx 5\sqrt{Z}\ \text{sec}^{-1}$$

Accordingly, the typical heating times of intermediate and heavy ions are 30–50 msec, which coincides with the ion loss rate in electron-beam ionizers.[87,94]

The relations given in the preceding section allow us to estimate the effect of the residual gas on the production of highly charged ions and the time for neutralization of the proper charge in the beam.

The residual-gas pressure in the KRION-2 ionizer is $\lesssim 1.3 \cdot 10^{-10}$ Pa (10^{-12} mm Hg).[87] Using the ionization cross sections from Ref. 30 and the charge exchange cross sections of Ref. 38 in (51), we conclude that in principle Xe^{54+} ions can be produced in this source and that the overall time for neutralization of N^{7+} ions from the residual gas is about 20 sec.

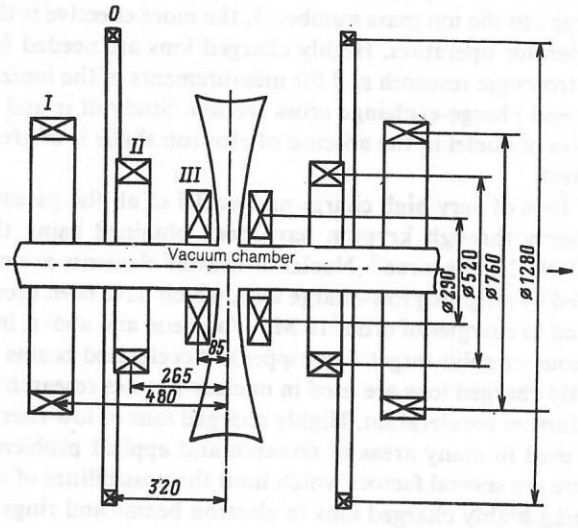

FIG. 11. Schematic depiction of the magnetic system of the adhesator of the JINR heavy-ion collective accelerator: 0–III—compression coils.

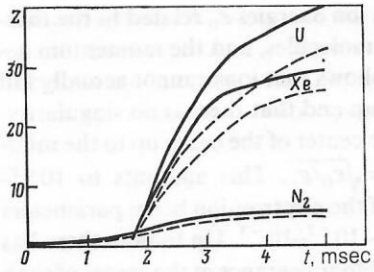

FIG. 12. Variation of the average charge of nitrogen, xenon, and uranium ions as a function of time in the electron ring of a collective accelerator: solid line—$N_e = 10^{13}$; dashed line—$N_e = 5 \cdot 10^{12}$.

Ion accumulation in electron rings

Let us consider ion accumulation in the electron rings of collective accelerators. As a rule, in the various types of circular electron accelerators a fairly good vacuum is created in order to make the number of ions produced insignificant.

In the HICAC electron rings are formed from a linear electron beam in a device called an adhesator.[9] The adhesator consists of a thin-walled chamber and a system of current-carrying coils of decreasing radius (Fig. 11). The electron beam is injected into a weakly focusing magnetic field and bent into a ring of radius 35 cm. The sequential switching on of the contraction coils causes the magnetic field to increase in time and compresses the ring. The electron energy is increased. There also exist methods of compressing electron rings in stationary spatially uniform magnetic fields.[100]

The electron rings obtained after compression at the JINR HICAC are characterized by the following parameters[9]:

Large radius R, cm: 3.5
Small rms radii a, cm: 0.1
Number of electrons: up to 10^{13}
Electron energy, MeV: 20.

The total time for the formation of the electron ring is 2–3 msec. In electron rings ions are produced from the residual gas or from specially injected jets of neutral gas. Various types of atom sources have been constructed. At the HICAC a gas-dynamic source is used to obtain pulsed fluxes of gaseous materials[101] and a laser source is used for solid materials.[102] In Fig. 12 we show the calculated variation of the average charge of nitrogen, xenon, and uranium atoms in the ring.[81] The neutral-atom source is switched on at time $t \approx 1.7$ msec when the ring radius is $R = 5$ cm. The solid lines correspond to a number of electrons equal to 10^{13} and the dashed lines to $5 \cdot 10^{12}$.

The electron density over the ring cross section obeys a Gaussian distribution:

$$\rho_e = \frac{N_e}{2\pi a_e^2} \exp\left(-\frac{r^2}{2a_e^2}\right). \tag{60}$$

Since the ring is quite narrow, all effects related to the curvature can be neglected in ion storage. Ion accumulation in nonuniformly charged beams has been studied in Refs. 85, 86, 98, 99, and 103–105.

In an electron beam with Gaussian density the ionization probability depends on the radius. For this reason, ions of different total energy will undergo further ionization with different probability. Low-energy ions located near the bottom of the potential well move in the center of the beam, where the electron density is a maximum, and have a relatively high probability of undergoing further ionization. High-energy ions spend a significant amount of time at the edge of the beam, where the electron density is low and, accordingly, the average ionization probability during an oscillation period is smaller. Therefore, the average energy of each new charge state will be lower than in the case of an electron beam of constant density and, accordingly, the rms dimensions and velocities will be smaller.

The electron distribution (60) has an intrinsic nonlinear electric field

$$F_e(r) = \frac{2eN_e}{r}\left(1 - \exp\left(-\frac{r^2}{2a_e^2}\right)\right). \tag{61}$$

However, most of the ions are produced and move at the center of the beam, where the fields are linear. We shall assume that all ions undergo harmonic oscillations with frequency $\omega_i = \sqrt{iN_e r_e m/AM}\,(c/a_e)$. Their total energy is $\varepsilon_i = AMv^2/2 + AMr^2\omega_i^2/2$. These assumptions were used in Refs. 98, 99, 104, and 105 to obtain stationary distribution functions for ions of any charge state with the condition that as a result of the production of each new charge state the distribution function of the preceding charge state is changed only slightly:

$$f_i = \frac{AMN_i}{2\pi^2 a_i^3 \omega_i} \exp\left(-\frac{r^2}{2a_i^2} - \frac{v^2}{2a_i^2\omega_i^2}\right) \delta(M_\varphi). \tag{62}$$

The approximate distribution functions for ions in the first few charge states in electron beams with Gaussian density were obtained in Ref. 106. The exact solution of the problem of finding the ion distribution function can be obtained by integrating the kinetic equation over the characteristics. This solution was obtained for ions of the first charge state in Ref. 86 and coincides with (62). After integrating the distribution function (62) over the ion velocities, it is easy to find the ion density in the beam cross section:

$$\rho_i = \sqrt{\frac{2}{\pi}} \frac{N_i}{2\pi a_i r} \exp(-r^2/2a_i^2). \tag{63}$$

Here, as in (54), the singularity at the center of a beam arises because the derivation of (63) did not include the ion initial velocities corresponding to the thermal motion of the neutral atoms.

The distribution function (62) has second-order moments corresonding to the rms sizes and velocities:

$$\left.\begin{aligned} a_i^2 &= a_1^2/i = a_e^2/2i; \\ v_i^2 &= a_i^2\omega_i^2 = a_1^2\omega_1^2 = \text{const}. \end{aligned}\right\} \tag{64}$$

The ion effective phase space is

$$E_i = a_i v_i = a_1^2 \omega_i / \sqrt{i} = E_1/\sqrt{i}. \tag{65}$$

The effect of the nonlinearity of the electron fields and the ion fields and also the variations in the ion distribution function in going from one charge state to another must be included by numerical modeling. The distribution-function moments method studied in Sec. 2 is an adequate approach for solving problems in charged-beam dynamics, including the case of multicomponent beams. However, the moments method involves the use of averaged quantities. The large-scale particle method can be used to study the detailed beam characteristics and the particle distribution functions or to take into account various types of nonlinearity.

The large-scale particle method amounts to the numerical solution of the kinetic equation over the characteristics[65,66] and allows the reproduction of all the electric, magnetic, and atomic interactions between particles in the beam. This method has been used to model storage processes and ion acceleration in electron beams and rings.[107–110] A small number of particles (several hundreds) was used in the calculations, which made it impossible to study electron–ion and ion–ion processes and the dynamics of the distribution functions or to treat several ion charge states simultaneously. To solve such problems, a program has been written for a computer comparable to the SDS-6500 which simultaneously treats up to 10 000 particles representing the electron and several ion components.[111,112]

The special feature of this program is the fact that the intrinsic fields of the electrons and ions U are determined on a grid in polar coordinates by solution of the Poisson equation $\Delta U = -4\pi\rho$ with boundary conditions, for example, $U|_{r=R} = 0$ and $\partial U/\partial r|_{r=0} = 0$, where R is the boundary of the region considered. The Poisson equation is solved by a fast Fourier transform.[113] We shall present the main results of the calculations, which are described in more detail in Refs. 98, 104, and 105. The dynamics of the rms dimensions and the effective phase spaces were studied as a function of the ion charge state (Fig. 13). Roughly 1000 particles were used to represent each ionic charge state. The electron distribution over the cross section is a Gaussian (60), and the intrinsic nonlinear electric field has the form (61). The fields produced by the ions were neglected. The calculations were carried out for two cases. In the first (case α), corresponding to the conditions under which the distribution function (62) was found, it was assumed that when new ions are produced the distribution function of the preceding charge state is left unchanged. The change of the distribution function was taken into account in case β.

In Fig. 14 we give the calculated density distribution as a function of the radius, averaged over circular layers of thickness $h_R = a_i/20$ and divided by the average density in the central region ρ_0 of radius $h_r/2$, for the first and tenth charge states in case α. The dashed lines in this figure show the ion and electron densities (63) and (60) averaged in the same manner for $a_e = \sqrt{2}a_i$ and $N_e = 10N_i$. The result of the numerical calculation is in very good agreement with the model distribution function (62). The density at the center of the beam ρ_0 is determined by the value of h_r and can be several tens of times larger than the electron density. The expression (63) and the analogous expression (54) for electron beams of constant density give a physically impossible infinite density at the center of the beam. The inclusion of the nonzero moments of the ion momenta,[97] whose values are determined by the initial ion energies ε_0 related to the thermal energy of the initial molecules, and the momentum acquired in the ionization shows that ions cannot actually fall into the center of the beam and that there is no singularity. The ion can approach the center of the beam up to the minimum distance $r_{\min}/a_i = \sqrt{\varepsilon_0/\varepsilon_i}$. This amounts to 10^{-3}–10^{-4} for typical values of the electron-ion beam parameters and, accordingly, $\rho_e/\rho_0 \sim 10^{-2}$–$10^{-3}$. Up to now there has been no study of the possible appearance at the center of such beams of electron-ion instabilities leading to a change of the distribution function (62) and an increase of the ion transverse phase space. It can be noted that the restrictions on the total number of ions at the center of the beam prevent the occurrence of large variations in the intrinsic fields and a large frequency shift. According to the estimates of Ref. 104, the ion distribution (62) noticeably affects the field at the center of the beam when the neutralization factor is $f \gtrsim \sqrt{\pi/2}\,(1/4\bar{\imath})$, where $\bar{\imath}$ is the average ion charge. In the case of long-term containment collisions of the ions with electrons and with each other at the center of the beam cause the ion distribution function to be transformed into a Boltzmann distribution, which has no singularities.

In Fig. 13(a) we show the variation of the ratio of the rms dimensions of ions of charge i to the rms dimensions of the electron beam, a_i/a_e. Figure 13(b) shows the ratio of the effective phase space of charge state i to the phase space of the first charge state in an electron beam of constant density. In these figures the curves labeled 1 are drawn through the points found using Eqs. (64) and (65) for a Gaussian electron beam density. The series of points show the results of numerical calculation using the nonlinear fields (61) for cases α and β. The accuracy of the numerical calculations can be judged from calculations of ion storage in an electron beam of constant density. The results of these calculations (shown by the crosses in Fig. 13) differ by no more than 1%–2% from the exact values found from Eqs. (59) and (60) and shown by the solid lines labeled 2. For singly charged ions the difference is less than 0.5%. The calculations were carried out for coincident rms dimensions and linear beam densities corresponding to the constant and the Gaussian distribution. The results lead to the conclusion that the nonlinearity of the intrinsic fields in the case of the Gaussian electron distribution has a noticeable effect only on the distribution function of ions in the first two charge states. In Fig. 15 we show the dependence of the electric field potential U on the radius for various values of the factor describing neutralization by ions f of the electron proper charge.[99,104,105] The appearance of a local maximum at the center of the beam can be attributed to the high ion density at the center predicted by the distribution function (62). As

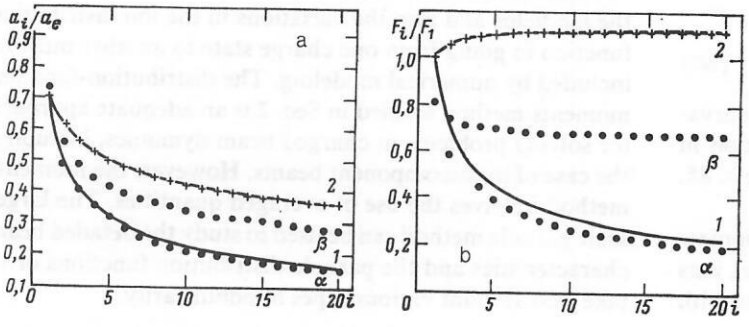

FIG. 13. Variation of the (a) rms dimensions and (b) effective phase space of the ion components as a function of the ion charge: 1—Gaussian beam density, calculation using the formulas (64); 2—uniform density of the electron beam, calculation using the formulas (55); the rows of points α and β correspond to numerical calculation using the large-scale particle method for two different modes of ion transitions between charge states in an electron beam with Gaussian density; the crosses correspond to the numerical calculation by the large-scale particle method for uniform density of the electron beam.

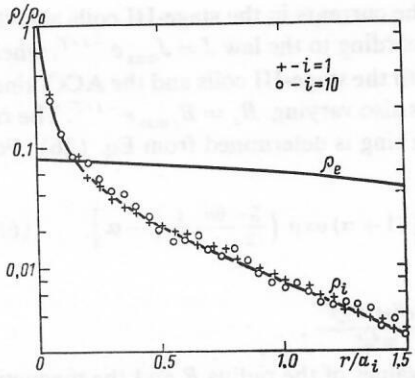

FIG. 14. Calculated dependence of the ion density on the radius for the first (+) and the tenth (○) charge state in an electron beam with Gaussian density.

the neutralization factor increases up to complete cancellation of the charge ($f = 1$), the ions are poorly confined by the electrons. The ion dimensions become larger than the electron ones, and the potential well does not completely disappear.

Comparing the features of ion storage in the cases of electron beams with uniform and Gaussian density, we note that in the latter case the rms dimensions and effective phase spaces of the ionic charge states fall off more rapidly with increasing ion charge. These results are particularly important for the collective acceleration of ions by electron rings, where there are rigorous requirements on the emittance of the ion beam as it leaves the accelerator.[12] The dynamics of the distribution functions and of the rms dimensions and velocities of electrons and ions of several charge states were also analyzed in Refs. 99, 104, and 105 as a function of the neutralization factor and the ion loss in charge-neutralized electron beams.

Possibilities of obtaining highly charged ions in the electron rings of collective accelerators

The ionization factor attainable at present in the electron rings of collective accelerators is $j\tau \approx 10^{20}$ cm^{-2}. This is sufficient for obtaining Xe^{20+} and U^{24+} ions (see Fig. 12). When the electron energy is relativistic, it is possible to ionize the inner shells of very heavy elements. In order to use electron rings to obtain highly charged ions, it is necessary to increase the electron-ring containment time.[89,114] The cross section for ionization by relativistic electrons of, for example, Xe^{53+} is $2\cdot10^{-23}$ cm^2, and for U^{89+} the cross section is $4\cdot10^{-23}$ cm^2 (Ref. 30). Therefore, an ionization factor of $j\tau \approx 10^{23}$ cm^{-2} is required to obtain xenon nuclei and helium-like ions of uranium. A ring with a number of electrons $N_e = 10^{13}$, radius $R = 3.5$ cm, and small rms radii $a = 1$–1.5 mm must be contained for at least 1 sec. In addition to the technical problems, this is prevented by energy losses of relativistic electrons to synchrotron radiation and by the increase of the small dimensions of the ring due to electron scattering on the stored ions. The power corresponding to the radiation losses is given by

$$\frac{d\varepsilon}{dt} = -\frac{2}{3}\frac{e^4 r_e}{m^3 c^5 R^2}. \qquad (66)$$

The characteristic time for the decrease of the electron energy due to synchrotron radiation for $\varepsilon = 20$ MeV is $\tau \approx 30$ msec.

In the case of electron-ion rings of small dimension there are two competing effects: decrease of the dimensions due to radiation friction and increase of the dimensions as a result of multiple electron scattering on the stored ions (37), (38).[115] These factors depend to a significant degree on the electron energy. For example, for the electron relativistic factor $\gamma = 30$–40 and ring radius $R \sim 4$ cm, the typical times of decrease of the dimensions due to synchrotron radiation are 30–60 msec, while those for the increase due to scattering are about 20–30 msec when the number of stored xenon ions is 10^{11}. Therefore, whereas in the early stage of the containment at large values of γ the radiation friction can compensate for electron scattering on the stored ions, as the electron energy decreases because of synchrotron radiation the scattering begins to dominate and the small dimensions grow rapidly. According to (5), (6), and (51), electron ring containment times of about 1 sec require a presently unattainable vacuum of $\lesssim 10^{-8}$ Pa in the chamber of the collective accelerator.[89] For the reasons discussed above, the containment time of the electron-ion rings of the HICAC is restricted to the range 50–100 msec. The maximum ion charge for constant ring dimensions is estimated to be $i = 46$–50 for xenon and $i = 74$–82 for uranium.

The production of ions of higher charge states requires a significant increase of the electron ring density. The electron rings are compressed in the magnetic field growing in time in the chamber of the adhesator. The final radius of the ring is $R_f \sim 1/\sqrt{B}$. The minimum value of the electron ring radius obtained at the HICAC is $R_f = 3$ cm for $B \simeq 25$ kOe (Ref. 116). Further decrease of the ring radius is limited by the magnetic system of the adhesator.

In Ref. 117 it was proposed that the electron synchrotron radiation be used for obtaining an additional compression of the electron ring. Owing to the synchrotron radiation, the radius decreases as

$$\frac{dR}{dt} = \frac{1}{1-n}\frac{R}{\varepsilon}\frac{d\varepsilon}{dt} = -\frac{2}{3(1-n)}\frac{r_e \varepsilon^3}{m^3 c^5 R^3}. \qquad (67)$$

Here n is the exponent of the magnetic field.

By producing a magnetic field with decay exponent close to unity at the final stage of the compression, it is possible to significantly decrease the ring radius with relatively small energy losses. Additional compression of the ring is accompanied by decreasing the electron energy, so large final values of the magnetic field are not required.

A calculation of the auxiliary compression system has

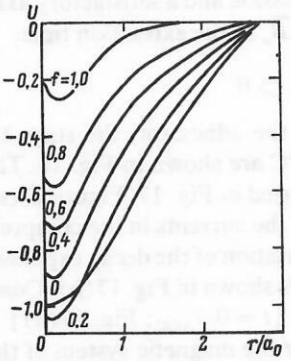

FIG. 15. Dependence of the electric field potential on the radius in an electron beam for various values of the factor describing electron charge neutralization by ions.

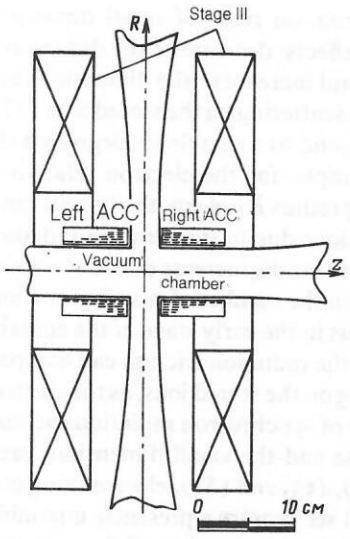

FIG. 16. Auxiliary compression system for the electron ring in the HICAC.

been carried out for the HICAC.[117] The necessary distribution of the magnetic field over the finite compression radii is ensured by the existing third compression coil and by auxiliary compression coils (ACC) (a system of current-carrying windings); see Fig. 16. After the usual compression the ring is located in a magnetic field with decay exponent close to unity. In the case of long-term containment of the ion ring the stage-III coils and the ACC are shorted out after the current reaches its maximum value.[118] The constant describing the decay time in the stage-III coil and the ACC is determined by the coil inductance and effective resistance and is about 50 msec. As a result, the radius of the electron ring is practically unchanged, since losses to synchrotron radiation compensate for the decrease of the guiding magnetic field. The variant of the auxiliary compression system is chosen on the basis of the following requirements:

(1) compression of the ring to the desired radius during a time of 5–10 msec for amplitude of the current in the ACC no greater than 10 kA;

(2) extraction of the compressed ring in the axial direction to the acceleration region (to a solenoid with decaying magnetic field), which puts a limit on the minimum radius of the windings.

These requirements are satisfied by a system of two coils, each with 20 windings of nonuniform pitch density, which ensures the necessary radial distribution of the magnetic field B_z during the compression and a satisfactory axial distribution of the mean value $\overline{B}_z$ at the extraction time:

$$\frac{1}{B_z}\left|\frac{\partial \overline{B}_z}{\partial z}\right| \leqslant 10^{-2}\,\text{cm}^{-1},\ B_r > 0.$$

The vacuum chamber of the adhesator, the stage-III compression coils, and the ACC are shown in Fig. 16. The operation of the setup is illustrated in Fig. 17. Figure 17(a) shows the time dependences of the currents in the compression coils and the ACC. The variation of the decay exponent along the trajectory of the ring is shown in Fig. 17(b). Compression to a radius of ~ 5 cm [$t = 0$–t_{ACC}; Fig. 17(a)] is effected in the usual manner by the magnetic system of the HICAC. After the current in the ACC is switched on the decay exponent n tends to its maximum value 0.97 [Fig. 17(b)]. The ring is rapidly compressed to 3 cm. After reaching their maxima the currents in the stage-III coils and the ACC are varied according to the law $J = J_{\max} e^{-t/T}$, where $T = 50$ msec for both the stage-III coils and the ACC, since the magnetic field is also varying: $B_z = B_{z\max} e^{-t/T}$. The radius of the electron ring is determined from Eq. (26). For $n \ll 1$, when $\overline{B}_z \approx B_z$:

$$R = R_0 \exp(3t/T) \Big/ \left[(1+\alpha)\exp\left(\frac{5-6n}{2-n}\,\frac{t}{T}\right) - \alpha\right], \qquad (68)$$

where

$$\alpha = \frac{4}{3(5-6n)}\,\frac{r_e R_0 e^3 B_{z_0}^3 T}{m^3 c^5},$$

R_0 and B_{z_0} are the values of the radius R and the magnetic field B_z at the initial stage of the long-term containment. The calculated variations of the parameters of the electron ring and of the beam of Xe and U ions are given in Table I (Ref. 115). The ring radius is given by (68). The small dimensions were found from Eq. (68) neglecting electron scattering on the ion. The presence in the ring of, for example, 10^{10} Xe ions causes the transverse dimensions of the ring to grow, making γ less than 10. This leads to an increase of the final small dimensions by roughly a factor of 1.5 compared to the values quoted. In Table I the time is measured from the instant at which formation of the electron ring begins.

It follows from (5) and (51) that in order to obtain Xe^{54+} ions during a time 0.1 sec the pressure of the residual gas in the accelerator chamber must be $\lesssim 10^{-7}$ Pa. An estimate using Eq. (59) shows that the characteristic time for ion heating due to collisions with electrons is ~ 0.1 sec.

The system that we have considered is a highly efficient source of highly charged ions and even nuclei of heavy elements. The source can operate on a cycle of about 1 Hz. The number of ions per cycle is restricted by the charge of the electron component and also by the possible increase of the small dimensions of the electron ring and amounts to 10^{10} Xe^{54+} ions and $3\cdot 10^9$ U^{90+} ions. The possibilities of obtaining xenon ions in the ERIS and other sources are illustrated in Fig. 18. The data on the PIG (a Penning-type plasma-arc source), DP (the duoplasmotron), and ECR (a source based on the electron-cyclotron resonance) are taken from Ref. 3. Sources of the ERIS type can be used to obtain ions of any elements, both gaseous substances and those which are solids under normal conditions.

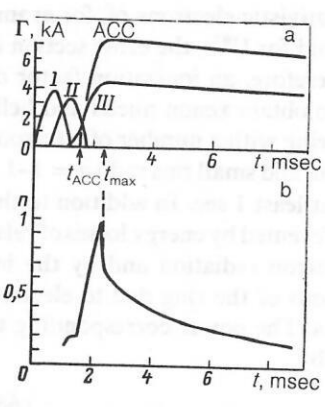

FIG. 17. Time dependences of the currents in the compression coils (I–III) and the ACC (a) and the exponent of the magnetic field decay accompanying the electron ring (b): t_{ACC}—time that the ACC is switched on; t_{max}—time corresponding to the maximum values of the currents in the stage-III coils and the ACC.

TABLE I. Parameters of the electron ring, the guiding magnetic field, the ionization factor, and the average charges of xenon and uranium ions in the ERIS as functions of the electron-ring containment time.

t, msec	R, cm	a, mm	ν	B, kOe	10^{22} cm^{-2}	z_{Xe}	z_U
2.5	3.5	1.0	50	20	0.01	20	24
7	2.0	0.8	35	29	0.25	42	68
15	1.5	0.7	23	26	1.0	51	83
30	1.3	0.7	15	20	3.5	53	86
60	1.5	1.0	9.3	11	8.5	54	89
100	2.4	1.5	6.1	5	12.5	54	90

CONCLUSIONS

The development of the collective method of acceleration using electron rings and the construction of electron-beam ion sources have stimulated detailed theoretical investigations into ion production and storage processes in electron beams and rings. As recently as 10–12 years ago it was difficult to reliably compute the number and average charge of the accumulated ions. In recent years several approaches have been developed which can be used to find the parameters of the ion component in electron beams and narrow rings. This has significantly aided the calculation and measurement of the ionization and charge exchange cross sections. At present it is possible to take into account the effect of various ionic charge states on each other and on the electron beam, the difference between the spatial distributions of these charge states, the nonlinearity of the intrinsic fields, and many other effects in multicomponent electron-ion beams. This has all been made possible by the development of the distribution function moments method in the physics of charged-particle beams. The second-order moments method has allowed the generalization of many earlier models and also the investigation of the effect of electron scattering on stored ions on the transverse dimensions of the electron and ion components. It has also made it possible to take into account effects related to the synchrotron radiation of relativistic electrons in circular beams. This method is particularly suited to the solution of various accelerator and beam problems using a computer. Even greater possibilities are opened up in the development of the moment method for obtaining approximately self-consistent equations for the higher-order moments.

In many cases the distribution functions of the various ionic charge states and their dependence on the ion charge are of interest. Numerical modeling based on the large-scale particle technique can be used successfully in this area.

The theoretical methods of describing processes in multicomponent electron beams and rings which have been discussed in this review lead, as a rule, to good agreement with the available experimental data. They can be used to guide the further development of electron-beam ion sources and also to investigate the possibility of designing a new type of ion source on the basis of the HICAC. Electron-beam sources are the most promising of the presently existing sources of very highly charged ions. When the energy of the electrons in the beam has been raised considerably and methods have been found to deal with ion losses, we can count on obtaining even higher charge states of ions of heavy elements.

The possibility of obtaining highly charged ions in electron rings is quite interesting. The principal merits of this source are as follows: a relativistic electron energy exceeding the energies of the inner shells of the heaviest elements; the predicted high intensity of the beam of highly charged ions; universality with regard to the type of chemical element ionized; the use of the same group of electrons throughout the entire ion stripping cycle.

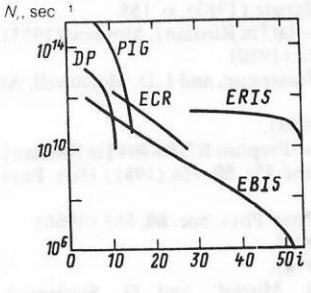

FIG. 18. Dependence of the yield of Xe ions on their charge state from various ion sources: PIG—plasma-arc source; DP—duoplasmotron; ECR—source based on the electron-cyclotron resonance; EBIS—electron-beam source; ERIS—ion source based on the electron ring of a collective accelerator.

APPENDIX

For beams with elliptically symmetric charge density

$$\rho=\rho\left(\frac{x^2}{a^2}+\frac{y^2}{b^2},\ t\right) \tag{A.1}$$

the electric field inside the beam can be found using the results of the theory of the Newton potential for ellipsoids with constant density.[119] The electric field strength is written as[68]

$$\left.\begin{aligned} E_x&=2\pi abx\int_0^\infty\frac{\rho\left(\frac{x^2}{a^2+s}+\frac{y^2}{b^2+s},\ t\right)ds}{(a^2+s)\,\Delta(s)};\\ E_y&=2\pi aby\int_0^\infty\frac{\rho\left(\frac{x^2}{a^2+s}+\frac{y^2}{b^2+s},\ t\right)ds}{(b^2+s)\,\Delta(s)};\\ \Delta(s)&=\sqrt{(a^2+s)(b^2+s)}. \end{aligned}\right\} \tag{A.2}$$

If $\rho(x, y)$ is a continuous function decreasing to zero at an infinite distance from the center of the beam, the field strength (A.2) and the corresponding potential also vanish at an infinite distance from the center of the distribution. We shall show that the expressions (A.2) imply that the equation div $\mathbf{E}=4\pi\rho$ is satisfied. For this we use the formulas

$$\left.\begin{aligned}&\frac{1}{(a^2+s)\,\Delta(s)}+\frac{1}{(b^2+s)\,\Delta(s)}=-2\frac{d}{ds}\frac{1}{\Delta(s)};\\&\left(\frac{x\frac{\partial}{\partial x}}{a^2+s}+\frac{y\frac{\partial}{\partial y}}{b^2+s}\right)\rho=2\left(\frac{x^2}{(a^2+s)^2}+\frac{y^2}{(b^2+s)^2}\right)\rho'=-2\frac{d\rho}{ds},\end{aligned}\right\}\tag{A.3}$$

where the prime in the second formula stands for differentiation with respect to the argument.

As a result we obtain

$$\operatorname{div}\mathbf{E}=2\pi ab\int_0^\infty\frac{d}{ds}\left[\frac{\rho\left(\frac{x^2}{a^2+s}+\frac{y^2}{b^2+s},\ t\right)}{\Delta(s)}\right]ds$$

$$=4\pi\rho\left(\frac{x^2}{a^2}+\frac{y^2}{b^2},\ t\right).\tag{A.4}$$

Therefore, the expressions (A.2) do actually represent the electric field strength inside a beam with a continuous, elliptically symmetric charge density which falls off to zero. Direct calculation using Eq. (A.1) gives the familiar expression for the electric field strength of a wire of elliptical cross section with radii a and b and constant density $\rho_0 = eN/\pi ab$:

$$E_x=4eN\frac{x}{a\,(a+b)};\quad E_y=4eN\frac{y}{b\,(a+b)}.\tag{A.5}$$

The expressions (A.2) are also valid for other bounded, elliptically symmetric density distributions.

In order to find the average value $\overline{xE}_x$ (or $\overline{yE}_y$), in the integral

$$\overline{xE}_x=\frac{2\pi ab}{N}\int_{-\infty}^{\infty}\int_{-\infty}^{\infty}dx\,dy\,\rho\left(\frac{x^2}{a^2}+\frac{y^2}{b^2}\right)\int_0^\infty\frac{ds\,\rho\left(\frac{x^2}{a^2+s}+\frac{y^2}{b^2+s}\right)}{(a^2+s)\,\Delta(s)}\tag{A.6}$$

we transform to new variables r and φ:

$$x=\sqrt{a^2+s}\,r\cos\varphi;\quad y=\sqrt{b^2+s}\,r\sin\varphi.\tag{A.7}$$

Performing the integration in (A.6), we obtain

$$\overline{xE}_x=eNa/(a+b)\tag{A.8}$$

and, accordingly, $\overline{yE}_y=eNb/(a+b)$ for an arbitrary integrable, elliptically symmetric density distribution.

This result, first obtained by Sacherer, remains valid when the ellipses are rotated relative to the coordinate axes. Then, as shown in Ref. 14, the average values (A.8) lead to the corresponding expressions for F_{sx} and b^s in Eqs. (19) and (20).

The matrix F_{sv} is found using the linear approximation for the electric field strength

$$F^s(x,\ \tau)=\varepsilon(x-\bar{x}),\tag{A.9}$$

where the matrix ε is the solution of the problem of minimizing the following functionals at a given instant of time:

$$D_i=\frac{1}{N}\int[\varepsilon_{i1}(x-\bar{x})+\varepsilon_{i2}(y-\bar{y})-F_i^s(x,\ y,\ t)]^2 f(Y,\ t)\,dY=\min,$$

$$i=1,\ 2.\tag{A.10}$$

Minimizing (A.10) using the formula for F_{sx} from (19), we obtain

$$\varepsilon=F_{sx}M_{xx}^{-1}=b^s\tag{A.11}$$

and the effective linearized force (21). Averaging of the effective force with weight v gives the force matrix F_{sv} in the form (19).

It was shown in Ref. 14 that the expression obtained for F_{sv} is exact (in spite of the linearization of the fields) for distribution functions which are elliptically symmetric in four-dimensional phase space, i.e., which are functions of a quadratic form of the type $(\tilde{Y}-\bar{\tilde{Y}})M^{-1}(Y-\bar{Y})$.

[1)]A similar closure was demonstrated for the three-dimensional problem in Ref. 70.

[1]G. N. Flerov, in: Nuclear Reactions at Low and Intermediate Energies, Proceedings of the All-Union Conference, Moscow, 1957 [in Russian], USSR Academy of Sciences, Moscow (1958), p. 489.
[2]A. M. Baldin, in: Ocherki po istorii razvitiya yadernoĭ fiziki v SSSR (Essays on the History of the Development of Nuclear Physics in the USSR), Naukova Dumka, Kiev (1982), p. 152.
[3]V. B. Kutner, Preprint R9-81-139 [in Russian], JINR, Dubna (1981).
[4]K. S. Golovanivskiĭ, At. Energ. **56**, 303 (1984).
[5]N. N. Venikov, in: Mezhdunarodnaya shkola molodykh uchenykh. Problemy uskoriteleĭ zaryazhennykh chastits (International School for Young Scientists: Charged Particle Accelerators), Preprint D9-12965 [in Russian], JINR, Dubna (1980), p. 121.
[6]E. D. Donets, USSR Inventor's Certificate No. 248860, "Methods of obtaining highly charged ions" [in Russian], Byull. OIPOTZ, No. 24 (1969).
[7]E. D. Donets, Fiz. Elem. Chastits At. Yadra **13**, 941 (1982) [Sov. J. Part. Nucl. **13**, 387 (1982)].
[8]V. I. Veksler, V. P. Sarantsev, A. G. Bonch-Osmolovsky *et al.*, in: Proc. of the Fourth Intern. Conf. on High Energy Accelerators, Cambridge, USA (1967), p. 289; Preprint R9-3440-2 [in Russian], JINR, Dubna (1968); At. Energ. **24**, 317 (1968).
[9]V. P. Sarantsev and É. A. Perel'shteĭn, Kollektivnoe uskorenie ionov élektronnymi kol'tsami (Collective Acceleration of Ions by Electron Rings), Atomizdat, Moscow (1979).
[10]É. A. Perel'shteĭn and G. D. Shirkov, in: Soveshchanie po problemam kollektivnogo metoda uskoreniya (Conference on Problems of the Method of Collective Acceleration), Preprint D9-82-664 [in Russian], JINR, Dubna (1982), p. 31.
[11]É. A. Perel'shteĭn and G. D. Shirkov, Preprint E9-85-4 [in English], JINR, Dubna (1985).
[12]V. S. Aleksandrov, P. F. Beloshitskiĭ, L. N. Belyaev *et al.*, "The JINR heavy-ion accelerator complex" [in Russian], Preprint R9-83-613, JINR, Dubna (1983).
[13]A. D. Dymnikov and É. A. Perel'shteĭn, Preprint R9-10620 [in Russian], JINR, Dubna (1977); Nucl. Instrum. Methods **148**, 567 (1978).
[14]N. Yu. Kazarinov, É. A. Perel'shteĭn, and V. F. Shevtsov, Preprint R9-10985 [in Russian], JINR, Dubna (1977); Part. Accel. **10**, 181 (1980).
[15]A. N. Didenko, V. N. Grigor'ev, and Yu. P. Usov, Moshchnye élektronnye puchki i ikh primenenie (High-Current Electron Beams and their Application), Atomizdat, Moscow (1977).
[16]C. L. Olson, Collective Ion Acceleration with Linear Electron Beams, Springer-Verlag, Berlin (1979), pp. 1–144.
[17]A. A. Rukhadze, L. S. Bogdankevich, S. E. Rosinskiĭ, and V. G. Rukhlin, Fizika sil'notochnykh relyativistskikh puchkov (Physics of High-Current Relativistic Beams), Atomizdat, Moscow (1980).
[18]K. Aleksander and W. Hintz, Fiz. Elem. Chastits At. Yadra **13**, 344 (1982) [Sov. J. Part. Nucl. **13**, 143 (1982)].
[19]V. M. Bystritskiĭ and A. N. Didenko, Fiz. Elem. Chastits At. Yadra **14**, 181 (1983) [Sov. J. Part. Nucl. **14**, 76 (1983)].
[20]G. Zschornack, Fiz. Elem. Chastits At. Yadra **14**, 835 (1983) [Sov. J. Part. Nucl. **14**, 349 (1983)].
[21]L. F. Presnyakov and R. K. Janev, in: Atomic Collision Processes with Multiply Charged Ions, Proceedings of the Second Workshop on the Vinča Accelerator Installation, Belgrade (1983), p. 155.
[22]A. A. Drozdovskiĭ, Preprint ITÉF-100 [in Russian], Moscow (1973).
[23]J. J. Thomson, Philos. Mag. **20**, 752 (1910).
[24]T. A. Carlson, C. W. Westor, N. Wasserman, and J. D. McDowell, At. Data **2**, 63 (1970).
[25]E. D. Donets, Phys. Scr. **T3**, 11 (1983).
[26]E. D. Donets and V. P. Ovsyannikov, Preprint R7-80-404 [in Russian], JINR, Dubna (1980); Zh. Eksp. Teor. Fiz. **80**, 916 (1981) [Sov. Phys. JETP **53**, 466 (1981)].
[27]M. H. Rudge and S. B. Schwarts, Proc. Phys. Soc. **88**, 563 (1966).
[28]A. Salop, Phys. Rev. A **8**, 3032 (1973).
[29]A. Salop, Phys. Rev. A **9**, 2496 (1974).
[30]Kh.-U. Zibert, D. Lemann, G. Muziol', and G. Shchornak, Soobshchenie (Communication) R9-10197, JINR, Dubna (1976).
[31]M. Cryzinski, Phys. Rev. **138**, A 336 (1965).
[32]C. L. Olson, Phys. Rev. A **11**, 288 (1975).
[33]R. K. Janev and L. P. Presnyakov, Phys. Rep. **70**, 1 (1981).
[34]R. K. Janev, in: Atomic Collision Processes with Multiply Charged

Ions, Proc. of the Second Workshop of the Vinča Accelerator Installation, Belgrade (1983), p. 37.
[35]T. Grosdanov, in: Atomic Collision Processes with Multiply Charged Ions. Proc. of the Second Workshop on the Vinča Accelerator Installation, Belgrade (1983), p. 53.
[36]S. Bleman, M. Bonnefoy, J. J. Bonnet *et al.*, Phys. Scr. **T3**, 63 (1983).
[37]A. Myuller and V. P. Shevel'ko, Zh. Tekh. Fiz. **50**, 985 (1980) [Sov. Phys. Tech. Phys. **25**, 593 (1980)].
[38]R. K. Janev and D. S. Belic, Phys. Scr. **T3**, 246 (1983).
[39]M. L. Iovnovich and M. M. Fiks, Preprint R9-4849 [in Russian], JINR, Dubna (1969); At. Energ. **29**, 429 (1970).
[40]V. George, M. L. Iovnovich, V. G. Novikov *et al.*, Soobshchenie (Communication) R9-6555, JINR, Dubna (1972).
[41]M. L. Iovnovich, A. B. Kuznetsov, and V. A. Preĭzendorf, Soobshchenie (Communication) R9-8119, JINR, Dubna (1974).
[42]D. Lemann, G. Myuller, G. Muziol', and G. Shchornak, Soobshchenie (Communication) R9-10744, JINR, Dubna (1977).
[43]B. Bochev, T. Kutsarova, and V. P. Ovsyannikov, Soobshchenie (Communication) R9-11566, JINR, Dubna (1978).
[44]É. A. Perel'shteĭn and G. D. Shirkov, Preprint R9-11412 [in Russian], JINR, Dubna (1978); Zh. Tekh. Fiz. **49**, 19 (1979) [Sov. Phys. Tech. Phys. **24**, 10 (1979)].
[45]V. D. Inkin, A. A. Mozelev, and V. P. Sarantsev, Soobshchenie (Communication) R9-12940, JINR, Dubna (1980).
[46]G. V. Dolbilov, V. D. Inkin, A. K. Krasnykh *et al.*, Soobshchenie (Communication) R9-12963, JINR, Dubna (1980).
[47]V. P. Sarantsev, V. D. Inkin, and A. A. Mozelev, Preprint R9-81-25 [in Russian], JINR, Dubna (1981).
[48]V. P. Sarantsev, V. D. Inkin, and A. A. Mozelev, Preprint R9-80-866 [in Russian], JINR, Dubna (1980).
[49]V. P. Sarantsev, V. D. Inkin, and A. A. Mozelev, Soobshchenie (Communication) R9-82-128, JINR, Dubna (1982).
[50]É. A. Perel'shteĭn, "Theory and calculation of collective acceleration of heavy ions," [in Russian], Author's Abstract of Doctoral Dissertation, 9-81-150, JINR, Dubna (1981).
[51]G. V. Dolbilov, V. I. Mironov, V. G. Novikov *et al.*, Soobshchenie (Communication) R9-11191, JINR, Dubna (1978).
[52]G. V. Dolbilov, V. I. Kazacha, I. V. Kozhukhov *et al.*, Soobshchenie (Communication) R9-12414, JINR, Dubna (1979).
[53]G. V. Dolbilov, A. K. Krasnykh, N. I. Lebedev *et al.*, Soobshchenie (Communication) R9-80-126, JINR, Dubna (1980).
[54]V. S. Aleksandrov, G. V. Dolbilov, I. V. Kuznetsov *et al.*, Soobshchenie (Communication) R9-83-862, JINR, Dubna (1983).
[55]N. Yu. Kazarinov, É. A. Perel'shteĭn, A. P. Sumbaev *et al.*, Soobshchenie (Communication) R9-81-428, JINR, Dubna (1981).
[56]N. Yu. Kazarinov, É. A. Perel'shteĭn, A. P. Sumbaev *et al.*, in: Trudy Soveshchaniya po problemam kollektivnogo metoda uskoreniya (Proceedings of the Conference on Problems of the Method of Collective Acceleration), D9-82-664, JINR, Dubna (1982), p. 16.
[57]G. N. Kulipapov and A. N. Skrinskiĭ, Usp. Fiz. Nauk **122**, 369 (1977) [Sov. Phys. Usp. **20**, 559 (1977)].
[58]B. Bochev, V. P. Ovsyannikov, and G. Kutsarova, Soobshchenie (Communication) R5-11567, JINR, Dubna (1978).
[59]E. D. Donets and V. P. Ovsyannikov, Soobshchenie (Communication) R7-10438, JINR, Dubna (1977).
[60]E. D. Donets, V. P. Ovsyannikov, and V. G. Dudnikov, Soobshchenie (Communication) R7-12905, JINR, Dubna (1978).
[61]G. D. Shirkov, Preprint R9-12055 [in Russian], JINR, Dubna (1978); Zh. Tekh. Fiz. **49**, 1471 (1979) [Sov. Phys. Tech. Phys. **24**, 818 (1979)].
[62]E. M. Lifshitz and L. P. Pitaevskiĭ, Fizicheskaya kinetika, Nauka, Moscow (1979); English translation: Physical Kinetics, Pergamon, Oxford (1981).
[63]I. M. Kapchinskiĭ, Teoriya lineĭnykh rezonansnykh uskoriteleĭ (Theory of Linear Resonance Accelerators), Energoizdat, Moscow (1982).
[64]J. D. Lawson, The Physics of Charged Particle Beams, Clarendon Press, Oxford (1977) [Russian translation published by Mir, Moscow (1980)].
[65]Vychislitel'nye metody v fizike plazmy (Computational Methods in Plasma Physics, Collection of Papers), Mir, Moscow (1974).
[66]A. S. Roshal', Modelirovanie zaryazhennykh puchkov (Modeling of Charged Beams), Atomizdat, Moscow (1979).
[67]P. M. Lapostolle, in: Proceedings of the Particle Accelerator Conf., Chicago, IEEE Trans. NS-18, Vol. 3 (1971), p. 1101.
[68]F. S. Sacherer, in: Proceedings of the Particle Accelerator Conference, Chicago, IEEE Trans. NS-18, Vol. 3 (1971), p. 1105.
[69]O. I. Yarkovoĭ, Preprint 2183 [in Russian], JINR, Dubna (1965); Zh. Tekh. Fiz. **36**, 988 (1966) [Sov. Phys. Tech. Phys. **11**, 731 (1966)].
[70]É. A. Perel'shteĭn and G. D. Shirkov, Preprint R9-10468 [in Russian], JINR, Dubna (1977); Zh. Tekh. Fiz. **48**, 249 (1978) [Sov. Phys. Tech. Phys. **23**, 149 (1978)].
[71]L. V. Bobyleva, N. Yu. Kazarinov, and É. A. Perel'shteĭn, Soobshchenie (Communication) Rll-81-796, JINR, Dubna (1981).
[72]E. P. Lee and R. K. Cooper, Part. Accel. **7**, 83 (1976).
[73]B. Bru and M. Weiss, CERN/MPS/LIN 72-4 (1972).
[74]P. N. Ostroumov, G. V. Romanov, and A. P. Fateev, Zh. Tekh. Fiz. **50**, 1237 (1980) [Sov. Phys. Tech. Phys. **25**, 710 (1980)].
[75]B. P. Murin, in: Tr. IV Vsesoyuznogo soveshchaniya po uskoritelyam zaryazhennykh chastits (Proceedings of the Fourth All-Union Conference on Charged Particle Accelerators), Vol. 1, Nauka, Moscow (1974), p. 123.
[76]G. N. Vyalov, N. Yu. Kazarinov, É. A. Perel'shteĭn *et al.*, Soobshchenie (Communication) R9-11672, JINR, Dubna (1978).
[77]O. I. Yarkovoĭ, Zh. Tekh. Fiz. **32**, 1285 (1962) [Sov. Phys. Tech. Phys. **7**, 951 (1963)].
[78]S. B. Rubin and O. I. Yarkovoĭ, Preprint 2882-2 [in Russian], JINR, Dubna (1966).
[79]N. Yu. Kazarinov, É. A. Perel'shteĭn and G. D. Shirkov, Zh. Tekh. Fiz. **50**, 549 (1980) [Sov. Phys. Tech. Phys. **25**, 330 (1980)].
[80]A. A. Kolomenskiĭ, Preprint 155 [in Russian], P. N. Lebedev Physics Institute, Moscow (1970); Fizicheskie osnovy metodov uskoreniya zaryazhennykh chastits (Physical Principles of Methods of Charged Particle Acceleration), Moscow State University Press, Moscow (1980).
[81]É. A. Perel'shteĭn and G. D. Shirkov, Soobshchenie (Communication) 9-80-124, JINR, Dubna (1980).
[82]R. J. Briggs, R. E. Hester, W. A. Lamb *et al.*, Bull. Am. Phys. Soc. **19**, 902 (1974).
[83]E. P. Lee, Phys. Fluids **19**, 60 (1976).
[84]V. S. Aleksandrov, G. V. Dolbilov, É. A. Perel'shteĭn *et al.*, Soobshchenie (Communication) 9-82-709, JINR, Dubna (1982).
[85]N. Yu. Kazarinov and É. A. Perel'shteĭn, Preprint R9-12441 [in Russian], JINR, Dubna (1979); Zh. Tekh. Fiz. **50**, 101 (1980) [Sov. Phys. Tech. Phys. **25**, 58 (1980)].
[86]N. Yu. Kazarinov, É. A. Perel'shteĭn, and G. D. Shirkov, Preprint R9-12719 [in Russian], JINR, Dubna (1979); Zh. Tekh. Fiz. **50**, 1722 (1980) [Sov. Phys. Tech. Phys. **25**, 1004 (1980)].
[87]E. D. Donets and V. P. Ovsyannikov, Preprint R7-80-515 [in Russian], JINR, Dubna (1980).
[88]F. Folkmann, R. Mann, and H. F. Beyer, Phys. Scr. **T3**, 88 (1983).
[89]É. A. Perel'shteĭn and G. D. Shirkov, in Soveshchanie po problemam kollektivnogo metoda uskoreniya OIYaI (Conference on the Problems of the Method of Collective Acceleration at JINR), D9-82-664, JINR, Dubna (1982), p. 31.
[90]A. B. Kuznetsov and V. A. Preĭzendorf, Soobshchenie (Communication) R9-80-820, JINR, Dubna (1980).
[91]V. G. Abdul'manov, I. I. Averbukh, V. L. Auslender *et al.*, in: Mezhdunarodnaya konferentsiya po uskoritelyam zaryazhennykh chastits vysokikh énergiĭ (International Conference on High Energy Charged Particle Accelerators), Vol. 1, Serpukhov (1977), p. 345.
[92]S. Arianer, C. Collart, Ch. Goldstein *et al.*, Phys. Scr. **13**, 35 (1983).
[93]R. Kenefick and R. Hamm, Preprint GSI-P-3-77 Darmstadt (1977).
[94]J. Faure, B. Feinberg, Antoine *et al.*, in: 12th Intern. Conf. on High Energy Accelerators, Fermilab, FNAL, Batavia (1983), p. 206.
[95]A. M. Baldin, E. D. Donets, I. B. Issinsky *et al.*, Phys. Scr. **T3**, 43 (1983).
[96]L. S. Laslett, Preprint ERAN-218, LBL Berkeley (1972).
[97]A. A. Drozdovskiĭ, Preprint ITÉF-10 [in Russian], Moscow (1973).
[98]É. A. Perel'shteĭn and G. D. Shirkov, Preprint R9-82-526 [in Russian], JINR, Dubna (1982).
[99]É. A. Perel'shteĭn, V. F. Shevtsov, G. D. Shirkov, and B. G. Shchinov, in: Trudy VIII Vsesoyuznogo sovechshaniya po uskoritelyam zaryazhennykh chastits (Proceedings of the Eighth All-Union Conference on Charged Particle Accelerators), Vol. II, Dubna (1983), p. 375.
[100]L. S. Barabash, P. F. Beloshitskiĭ, N. Yu. Kazarinov *et al.*, Soobshchenie (Communication) R9-11776, JINR, Dubna (1978).
[101]V. G. Novikov, V. P. Sarantsev, Z. A. Ter-Martirosyan, and B. A. Shestakov, in: Soveshchanie po problemam kollektivnogo metod uskoreniya (Conference on Problems of the Method of Collective Acceleration), D9-82-664, JINR, Dubna (1982), p. 23.
[102]Yu A. Bykovskiĭ, V. P. Sarantsev, S. M. Sil'nov *et al.*, in: Soveshchanie po problemam kollektivnogo metoda uskoreniya (Conference on Problems of the Method of Collective Acceleration), D9-82-664, JINR, Dubna (1982), p. 27.
[103]I. Hofman, Preprint IPP 0/21, IPP, Garching (1974).
[104]É. A. Perel'shteĭn, V. F. Shevtsov, G. D. Shirkov, and B. G. Shchinov, Preprint R9-82-532 [in Russian], JINR, Dubna (1982).
[105]É. A. Perel'shteĭn, V. F. Shevtsov, G. D. Shirkov, and B. G. Shchinov, Zh. Tekh. Fiz. **54**, 270 (1984) [Sov. Phys. Tech. Phys. **29**, 158 (1984)].
[106]A. B. Kuznetsov, Preprint R9-83-349 [in Russian], JINR, Dubna (1983).
[107]E. A. Perel'shteĭn, V. F. Shevtsov, and B. G. Shchinov, Preprint R9-10060 [in Russian], JINR, Dubna (1976).
[108]V. S. Aleksandrov, G. V. Dolbilov, N. Yu. Kazarinov *et al.*, Soobsh-

chenie (Communication) R9-11949, JINR, Dubna (1978).
[109]N. Yu. Kazarinov, V. I. Kazacha, É. A. Perel'shteĭn *et al.*, Soobshchenie (Communication) R9-12720, JINR, Dubna (1979).
[110]V. S. Aleksandrov, Yu. I. Aleksakhin, N. Yu. Kazarinov *et al.*, Soobshchenie (Communication) R9-80-368, JINR, Dubna (1980).
[111]É. A. Perel'shteĭn, V. F. Shevtsov, G. D. Shirkov, and B. G. Shchinov, in: Programmirovanie i matematicheskie metody resheniya fizicheskikh zadach (Programning and Mathematical Methods of Solving Physical Problems), D10,11-84-818, JINR, Dubna (1985), p. 204.
[112]É. A. Perel'shteĭn, G. D. Shirkov, and B. G. Shchinov, Preprint 11-84-505 [in Russian], JINR, Dubna (1984); in: Chislennye metody i prilozheniya (Numerical Methods and Applications), Sofiya (1985), p. 471.
[113]S. P. Christiansen and R. W. Hockny, Comput. Phys. Commun. **2**, 139 (1971).
[114]D. Kif, in: Tr. IV Vsesoyuznogo soveshchaniya po uskoritalyam zaryazhennykh chastits (Proceedings of the Fourth All-Union Conference on Charged particle Accelerators), Vol. 1, Nauka, Moscow (1975), p. 109.
[115]É. A. Perel'shteĭn and G. D. Shirkov, Preprint E9-85-4 [in English], JINR, Dubna (1985).
[116]V. P. Sarantsev, V. S. Aleksandrov, L. S. Barabash *et al.*, Soobshchenie (Communication) R9-10917, JINR, Dubna (1977).
[117]V. S. Aleksandrov, É. A. Perel'shteĭn, V. P. Sarantsev, and G. D. Shirkov, Soobshchenie (Communication) R9-81-20, JINR, Dubna (1981).
[118]V. G. Novikov and É. A. Perel'shteĭn, USSR Inventor's Certificate No. 766384, "Methods of obtaining highly charged ions" [in Russian], No. 4, Izobreteniya, Otkrytiya (1983).
[119]L. N. Sretenskiĭ, Teoriya n'yutonovskogo potentsiala (Theory of the Newton Potential), Gostekhteorizdat, Moscow–Leningrad (1946).

Translated by Patricia Millard